10.7.5.1 Human Estimates

Tables 10-19 through 10-24 present the regional deposition fractions (% deposition) and regional deposited particle mass (μg) for each of the three ambient human exposure aerosols depicted in Figures 10C-1, 10C-2a (Philadelphia), and 10C-2b (Phoenix). Data are shown for normal augmenters (Tables 10-19, 10-21, and 10-23) versus mouth breathers (Tables 10-20, 10-22, and 10-24) for three different activity patterns.

TABLE 10-19. DAILY MASS DEPOSITION OF PARTICLES FROM AEROSOL DEFINED IN FIGURE 10C-1 IN THE RESPIRATORY TRACT OF "NORMAL AUGMENTER" ADULT MALE HUMANS EXPOSED TO A PARTICLE MASS CONCENTRATION OF 50 μg/m^3

		Contribution to Total Deposited Particle Mass from Each Aerosol Mode[a]					
		Nuclei Mode		Accumulation Mode		Coarse Mode	
Activity Pattern	Region of Respiratory Tract	Percent Deposited[b]	Mass of Particles (μg)	Percent Deposition	Mass of Particles (μg)	Percent Deposition	Mass of Particles (μg)
General population[c]	ET$_1$	1.0	10	0.7	7	16.3	162
	ET$_2$	1.1	11	0.7	7	19.0	189
	BB	0.4	4	0.2	2	0.9	9
	bb	2.4	24	1.1	11	0.7	7
	AI	7.0	69	4.2	42	2.5	25
	Total	11.7	117	6.8	68	39.4	392
Workers, light work[d]	ET$_1$	0.9	10	0.7	8	15.4	176
	ET$_2$	1.1	12	0.7	8	19.2	220
	BB	0.3	4	0.2	2	1.5	18
	bb	2.2	26	1.0	11	0.8	9
	AI	7.2	82	4.1	47	2.4	28
	Total	11.7	134	6.6	76	39.4	451
Workers, heavy work[e]	ET$_1$	0.8	11	0.7	9	8.8	117
	ET$_2$	1.0	14	0.7	9	20.0	267
	BB	0.3	4	0.2	2	6.0	80
	bb	2.1	29	0.9	12	1.2	16
	AI	7.4	98	4.0	54	2.7	36
	Total	11.7	156	6.5	87	38.6	517

[a]Nuclei mode MMAD = 0.0169 μm, σ_g = 1.6, density = 1.4 g/cm^3, 15.6% of the aerosol mass; accumulation mode MMAD = 0.180 μm, σ_g = 1.8, density = 1.2 g/cm^3, 38.7% of the aerosol mass; coarse mode MMAD = 5.95 μm, σ_g = 1.87, density = 2.2 g/cm^3, 45.7% of the aerosol mass (see Tables 10C-1 and 10C-2c).

[b]Expressed as a percentage of the total mass of particles in the volume of ambient air inhaled.

[c]Average for 24 h, as derived from ICRP-66 (1994): for 33.3% sleep, 33.3% sitting, and 33.3% light exercise (see Table 10B-1).

[d]Average for 24 h, as derived from ICRP-66 (1994): for 33.3% sleep, 27.1% sitting, and 35.4% light exercise, 4.2% heavy exercise (see Table 10B-1).

[e]Average for 24 h, as derived from ICRP-66 (1994): for 33.3% sleep, 16.7% sitting, and 41.7% light exercise, 8.3% heavy exercise. (see Table 10B-1).

TABLE 10-20. DAILY MASS DEPOSITION OF PARTICLES FROM AEROSOL DEFINED IN FIGURE 10C-1 IN THE RESPIRATORY TRACT OF "MOUTH BREATHER" ADULT MALE HUMANS EXPOSED TO A PARTICLE MASS CONCENTRATION OF 50 μg/m^3

		Contribution to Total Deposited Particle Mass from Each Aerosol Mode[a]					
		Nuclei Mode		Accumulation Mode		Coarse Mode	
Activity Pattern	Region of Respiratory Tract	Percent Deposited[b]	Mass of Particles (μg)	Percent Deposition	Mass of Particles (μg)	Percent Deposition	Mass of Particles (μg)
General population[c]	ET$_1$	0.5	5	0.3	3	7.3	72
	ET$_2$	1.1	11	0.5	5	16.2	162
	BB	0.4	4	0.2	2	4.2	42
	bb	2.4	24	1.1	11	2.1	21
	AI	7.2	71	4.2	42	6.2	62
	Total	11.6	116	6.3	63	36.0	358
Workers, light work[d]	ET$_1$	0.5	6	0.3	3	6.8	78
	ET$_2$	1.1	12	0.5	6	16.8	192
	BB	0.4	4	0.2	2	4.8	55
	bb	2.3	26	1.0	11	2.1	24
	AI	7.4	84	4.1	47	5.8	66
	Total	11.6	133	6.1	70	36.3	415
Workers, heavy work[e]	ET$_1$	0.5	6	0.3	4	6.4	86
	ET$_2$	1.0	14	0.5	7	17.2	230
	BB	0.3	4	0.2	2	5.4	72
	bb	2.2	29	0.9	12	2.0	27
	AI	7.5	101	4.1	54	5.4	73
	Total	11.6	155	5.9	79	36.5	488

[a]Nuclei mode MMAD = 0.0169 μm, σ_g = 1.6, density = 1.4 g/cm^3, 15.6% of the aerosol mass; accumulation mode MMAD = 0.180 μm, σ_g = 1.8, density = 1.2 g/cm^3, 38.7% of the aerosol mass; coarse mode MMAD = 5.95 μm, σ_g = 1.87, density = 2.2 g/cm^3, 45.7% of the aerosol mass (see Tables 10C-1 and 10C-2c).

[b]Expressed as a percentage of the total mass of particles in the volume of ambient air inhaled.

[c]Average for 24 h, as derived from ICRP-66 (1994): for 33.3% sleep, 33.3% sitting, and 33.3% light exercise. (See Table 10B-1).

[d]Average for 24 h, as derived from ICRP-66 (1994): for 33.3% sleep, 27.1% sitting, and 35.4% light exercise, 4.2% heavy exercise. (See Table 10B-1).

[e]Average for 24 h, as derived from ICRP-66 (1994): for 33.3% sleep, 16.7% sitting, and 41.7% light exercise, 8.3% heavy exercise. (See Table 10B-1).

TABLE 10-21. DAILY MASS DEPOSITION OF PARTICLES FROM PHILADELPHIA AEROSOL DEFINED IN FIGURE 10C-2(a) IN THE RESPIRATORY TRACT OF "NORMAL AUGMENTER" ADULT MALE HUMANS EXPOSED TO A PARTICLE MASS CONCENTRATION OF 50 μg/m^3

		Contribution to Total Deposited Particle Mass from Each Aerosol Mode[a]					
		Accumulation Mode		Intermodal Mode		Coarse Mode	
Activity Pattern	Region of Respiratory Tract	Percent Deposited[b]	Mass of Particles (μg)	Percent Deposition	Mass of Particles (μg)	Percent Deposition	Mass of Particles (μg)
General population[c]	ET$_1$	2.0	19	1.9	19	13.0	130
	ET$_2$	1.9	19	2.6	26	13.4	134
	BB	0.2	2	0.2	2	0.2	2
	bb	0.7	7	0.2	2	0.1	1
	AI	3.7	37	1.1	11	0.1	1
	Total	8.5	84	6.0	60	26.8	267
Workers, light work[d]	ET$_1$	1.9	22	1.8	21	12.2	139
	ET$_2$	1.9	22	2.6	30	14.2	162
	BB	0.2	2	0.2	3	0.3	3
	bb	0.6	7	0.2	2	0.1	1
	AI	3.6	42	1.1	13	0.1	1
	Total	8.3	95	5.9	68	26.8	307
Workers, heavy work[e]	ET$_1$	1.9	26	1.8	24	11.6	156
	ET$_2$	2.0	26	2.6	35	14.7	197
	BB	0.2	3	0.3	4	0.3	5
	bb	0.6	8	0.2	2	0.1	1
	AI	3.6	48	1.1	14	0.1	1
	Total	8.3	111	6.0	80	26.8	359

[a]Accumulation mode MMAD = 0.436 μm, σ_g = 1.51, density = 1.3 g/cm^3, 48.2% of the aerosol mass; intermodal mode MMAD = 2.20 μm, σ_g = 1.16, density = 1.3 g/cm^3, 7.4% of the aerosol mass; coarse mode MMAD = 28.8 μm, σ_g = 2.16, density = 1.3 g/cm^3, 44.4% of the aerosol mass (see Tables 10C-3 and 10C-4c).

[b]Expressed as a percentage of the total mass of particles in the volume of ambient air inhaled.

[c]Average for 24 h, as derived from ICRP-66 (1994): for 33.3% sleep, 33.3% sitting, and 33.3% light exercise. (See Table 10B-1).

[d]Average for 24 h, as derived from ICRP-66 (1994): for 33.3% sleep, 27.1% sitting, and 35.4% light exercise, 4.2% heavy exercise. (See Table 10B-1).

[e]Average for 24 h, as derived from ICRP-66 (1994): for 33.3% sleep, 16.7% sitting, and 41.7% light exercise, 8.3% heavy exercise. (See Table 10B-1).

TABLE 10-22. DAILY MASS DEPOSITION OF PARTICLES FROM PHILADELPHIA AEROSOL DEFINED IN FIGURE 10C-2(a) IN THE RESPIRATORY TRACT OF "MOUTH BREATHER" ADULT MALE HUMAN EXPOSED TO A PARTICLE MASS CONCENTRATION OF 50 μg/m^3

		Contribution to Total Deposited Particle Mass from Each Aerosol Mode[a]					
		Accumulation Mode		Intermodal Mode		Coarse Mode	
Activity Pattern	Region of Respiratory Tract	Percent Deposited[b]	Mass of Particles (μg)	Percent Deposition	Mass of Particles (μg)	Percent Deposition	Mass of Particles (μg)
General population[c]	ET$_1$	0.5	5	0.7	7	6.6	66
	ET$_2$	0.6	6	1.0	10	18.3	182
	BB	0.2	2	0.3	3	1.1	11
	bb	0.7	7	0.3	3	0.2	2
	AI	3.9	39	1.9	19	0.4	4
	Total	5.9	59	4.2	42	26.6	265
Workers, light work[d]	ET$_1$	0.5	6	0.6	7	6.1	70
	ET$_2$	0.6	7	1.1	12	18.8	215
	BB	0.2	2	0.4	5	1.1	13
	bb	0.7	8	0.3	3	0.2	3
	AI	3.8	43	1.8	21	0.3	4
	Total	5.8	66	4.2	48	26.7	305
Workers, heavy work[e]	ET$_1$	0.5	7	0.6	8	5.7	76
	ET$_2$	0.6	8	1.1	15	19.3	259
	BB	0.2	3	0.5	6	1.2	16
	bb	0.6	8	0.3	4	0.2	3
	AI	3.7	50	1.8	24	0.3	4
	Total	5.7	76	4.3	57	26.7	357

[a]Accumulation mode MMAD = 0.436 μm, σ_g = 1.51, density = 1.3 g/cm^3, 48.2% of the aerosol mass; intermodal mode MMAD = 2.20 μm, σ_g = 1.16, density = 1.3 g/cm^3, 7.4% of the aerosol mass; coarse mode MMAD = 28.8 μm, σ_g = 2.16, density = 1.3 g/cm^3, 44.4% of the aerosol mass (see Tables 10C-3 and 10C-4c).

[b]Expressed as a percentage of the total mass of particles in the volume of ambient air inhaled.

[c]Average for 24 h, as derived from ICRP-66 (1994): for 33.3% sleep, 33.3% sitting, and 33.3% light exercise. (See Table 10B-1).

[d]Average for 24 h, as derived from ICRP-66 (1994): for 33.3% sleep, 27.1% sitting, and 35.4% light exercise, 4.2% heavy exercise. (See Table 10B-1).

[e]Average for 24 h, as derived from ICRP-66 (1994): for 33.3% sleep, 16.7% sitting, and 41.7% light exercise, 8.3% heavy exercise. (See Table

TABLE 10-23. DAILY MASS DEPOSITION OF PARTICLES FROM PHOENIX AEROSOL DEFINED IN FIGURE 10C-2(b) IN THE RESPIRATORY TRACT OF "NORMAL AUGMENTER" ADULT MALE HUMAN EXPOSED TO A PARTICLE MASS CONCENTRATION OF 50 μg/m^3

		Contribution to Total Deposited Particle Mass from Each Aerosol Mode[a]					
		Accumulation Mode		Intermodal Mode		Coarse Mode	
Activity Pattern	Region of Respiratory Tract	Percent Deposited[b]	Mass of Particles (μg)	Percent Deposition	Mass of Particles (μg)	Percent Deposition	Mass of Particles (μg)
General population[c]	ET$_1$	0.4	4	2.9	29	20.3	202
	ET$_2$	0.4	4	3.8	38	21.9	218
	BB	0.1	1	0.2	2	0.6	6
	bb	0.7	7	0.3	3	0.4	4
	AI	2.7	26	1.7	17	1.2	12
	Total	4.2	42	8.9	89	44.4	441
Workers, light work[d]	ET$_1$	0.4	4	2.8	32	19.1	218
	ET$_2$	0.4	4	3.8	43	22.8	260
	BB	0.1	1	0.3	4	1.0	11
	bb	0.6	7	0.3	3	0.4	4
	AI	2.6	30	1.7	19	1.2	13
	Total	4.1	47	8.9	101	44.3	507
Workers, heavy work[e]	ET$_1$	0.4	5	2.8	37	18.3	244
	ET$_2$	0.4	5	3.8	51	23.4	313
	BB	0.1	1	0.4	6	1.3	17
	bb	0.6	8	0.3	4	0.4	5
	AI	2.6	34	1.6	22	1.1	14
	Total	4.0	53	8.9	119	44.4	594

[a]Accumulation mode MMAD = 0.188 μm, σ_g = 1.54, density = 1.7 g/cm^3, 22.4% of the aerosol mass; intermodal mode MMAD = 1.70 μm, σ_g = 1.9, density = 1.7 g/cm^3, 13.8% of the aerosol mass; coarse mode MMAD = 16.4 μm, σ_g = 2.79, density = 1.7 g/cm^3, 63.9% of the aerosol mass (see Tables 10C-5 and 10C-6c).

[b]Expressed as a percentage of the total mass of particles in the ambient air inhaled.

[c]Average for 24 h, as derived from ICRP-66 (1994): for 33.3% sleep, 33.3% sitting, and 33.3% light exercise. (See Table 10B-1).

[d]Average for 24 h, as derived from ICRP-66 (1994): for 33.3% sleep, 27.1% sitting, and 35.4% light exercise, 4.2% heavy exercise. (See Table 10B-1).

TABLE 10-24. DAILY MASS DEPOSITION OF PARTICLES FROM PHOENIX AEROSOL DEFINED IN FIGURE 10C-2(b) IN THE RESPIRATORY TRACT OF "MOUTH BREATHER" ADULT MALE HUMANS EXPOSED TO A PARTICLE MASS CONCENTRATION OF 50 μg/m^3

		Contribution to Total Deposited Particle Mass from Each Aerosol Mode[a]					
		Accumulation Mode		Intermodal Mode		Coarse Mode	
Activity Pattern	Region of Respiratory Tract	Percent Deposited[b]	Mass of Particles (μg)	Percent Deposition	Mass of Particles (μg)	Percent Deposition	Mass of Particles (μg)
General population[c]	ET$_1$	0.2	2	1.0	10	9.8	98
	ET$_2$	0.3	3	1.7	17	25.5	254
	BB	0.1	1	0.5	5	3.1	31
	bb	0.7	7	0.5	5	1.2	12
	AI	2.7	27	2.7	27	3.0	30
	Total	4.0	40	6.4	63	42.7	425
Workers, light work[d]	ET$_1$	0.2	2	1.0	11	9.2	105
	ET$_2$	0.3	4	1.7	20	26.3	301
	BB	0.1	1	0.6	7	3.4	39
	bb	0.6	7	0.5	5	1.1	13
	AI	2.6	30	2.6	30	2.8	31
	Total	3.9	44	6.4	73	42.8	490
Workers, heavy work[e]	ET$_1$	0.2	2	1.0	13	8.5	114
	ET$_2$	0.3	4	1.8	24	27.0	362
	BB	0.1	1	0.8	10	3.7	50
	bb	0.6	8	0.4	6	1.1	14
	AI	2.6	35	2.5	34	2.6	34
	Total	3.8	50	6.5	86	42.9	574

[a]Accumulation mode MMAD = 0.188 μm, σ_g = 1.54, density = 1.7 g/cm^3, 22.4% of the aerosol mass; intermodal mode MMAD = 1.70 μm, σ_g = 1.9, density = 1.7 g/cm^3, 13.8% of the aerosol mass; coarse mode MMAD = 16.4 μm, σ_g = 2.79, density = 1.7 g/cm^3, 63.9% of the aerosol mass (see Tables 10C-5 and 10C-6c).

[b]Expressed as a percentage of the total mass of particles in the volume of ambient air inhaled.

[c]Average for 24 h, as derived from ICRP-66 (1994): for 33.3% sleep, 33.3% sitting, and 33.3% light exercise. (See Table 10B-1).

[d]Average for 24 h, as derived from ICRP-66 (1994): for 33.3% sleep, 27.1% sitting, and 35.4% light exercise, 4.2% heavy exercise. (See Table 10B-1).

[e]Average for 24 h, as derived from ICRP-66 (1994): for 33.3% sleep, 16.7% sitting, and 41.7% light exercise, 8.3% heavy exercise. (See Table 10B-1).

Recall from Section 10.4 that deposition of a particular aerosol (MMAD and σ_g) in the respiratory tract is a function of inhalability and deposition efficiency. This is illustrated schematically in Figure 10-39. The inhalability function (Figure 10-39b) for a specific respiratory tract region (or for the total respiratory tract as depicted in the figure) is integrated with the deposition efficiency function (Figure 10-39c). These are integrated with an aerosol characterized by its particle diameter and mass distribution data (Figure 10-39a) to estimate the mass deposition fraction (Figure 10-39d) in that region.

As expected from experimental studies, these simulations predict different deposition fractions for mouth breathing versus nasal breathing. This is most noticeable for deposition of the intermodal and coarse modes of the Philadelphia and Phoenix aerosols (depicted in Figures 10C-2a and 10C-2b), which showed significant increases in BB and AI deposition fractions. The MMAD for the intermodal and coarse modes were 2.20 and 28.8, respectively, for the Philadelphia aerosol; and 1.70 and 16.4, respectively, for the Phoenix aerosol. Deposition in these regions of the accumulation mode was less effected by mouth breathing as would be anticipated for these smaller MMADs.

Activity pattern influenced the deposition fractions greatly. ET deposition of all three modes increased with the ventiliation rates associated with work activity patterns. A noticeable increase in both BB and A deposition occurred with percent changes of increased deposition ranging up to 60%. Differences were also apparent in the nuclei and accumulation modes. For the aerosol depicted in Figure 10C-1, the nuclei mode (MMAD = 0.0169 μm), deposition fractions decreased in the bb and AI regions with the heavy work activity pattern compared to that for the general population. For the Philadelphia aerosol, deposition of the accumulation mode (MMAD = 0.436 μm) stayed the same in the BB region but decreased slightly in the bb and A regions with the heavy work activity pattern. For the Phoenix aerosol, deposition of the accumulation mode (MMAD = 0.188) increased in the bb and A compartments with the heavy work activity pattern. Figures 10-40 and 10-41 show the daily mass deposition (μg/d) predicted for normal augmenters versus mouth breathers and these different minute volume activity patterns for the Philadelphia and Phoenix aerosols, respectively.

Differences among the aerosols were also apparent and reflected the differences in the MMAD values and percent mass of each mode. Table 10-25 presents summary data for each

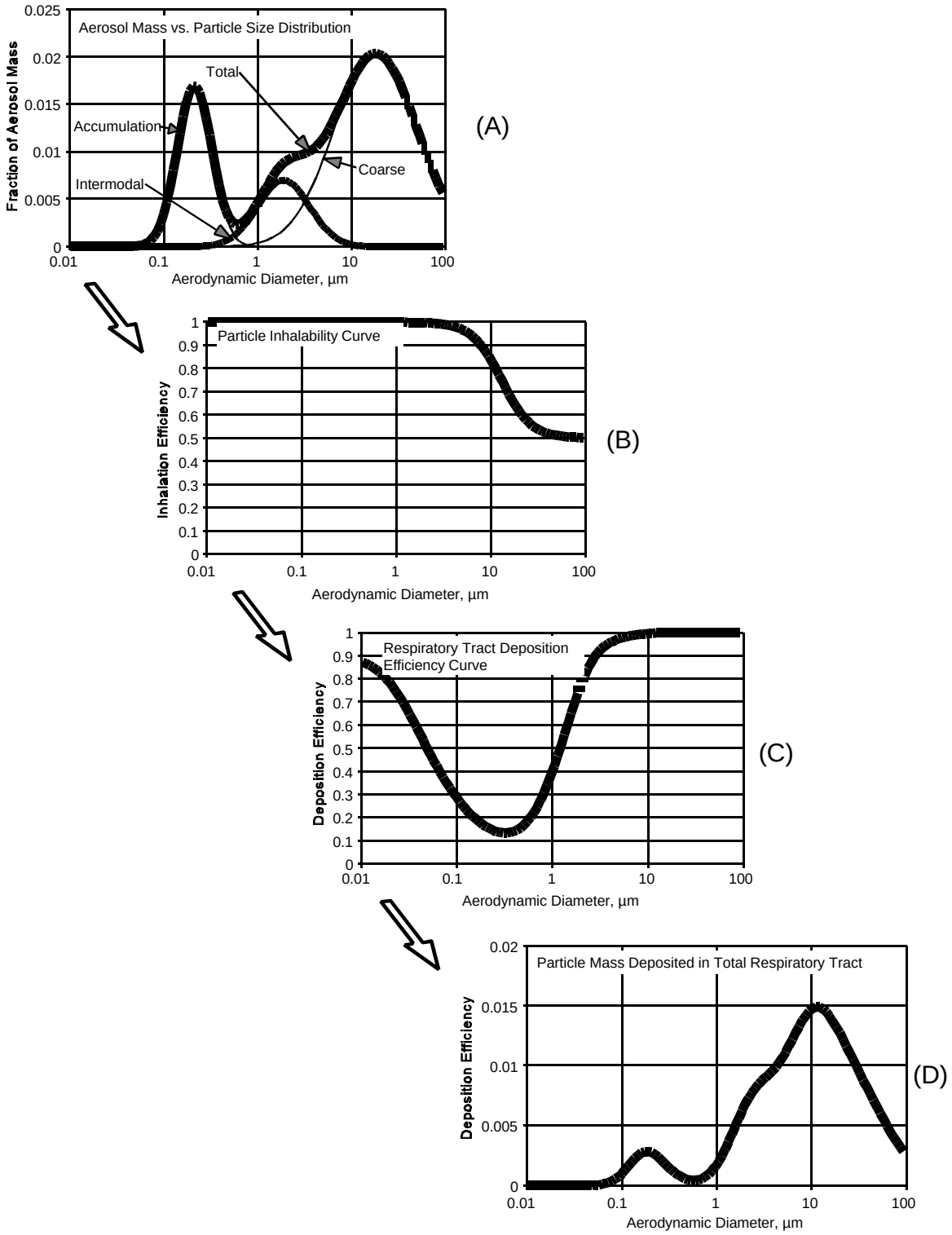

Figure 10-39. Schematic showing integration of inhalability (b) with deposition efficiency (c) functions. These functions are integrated with particle diameter and distribution data (a) to estimate deposition fractions of particle mass in each region of the respiratory tract (d). The particle mass fraction deposited in the total respiratory tract is illustrated.

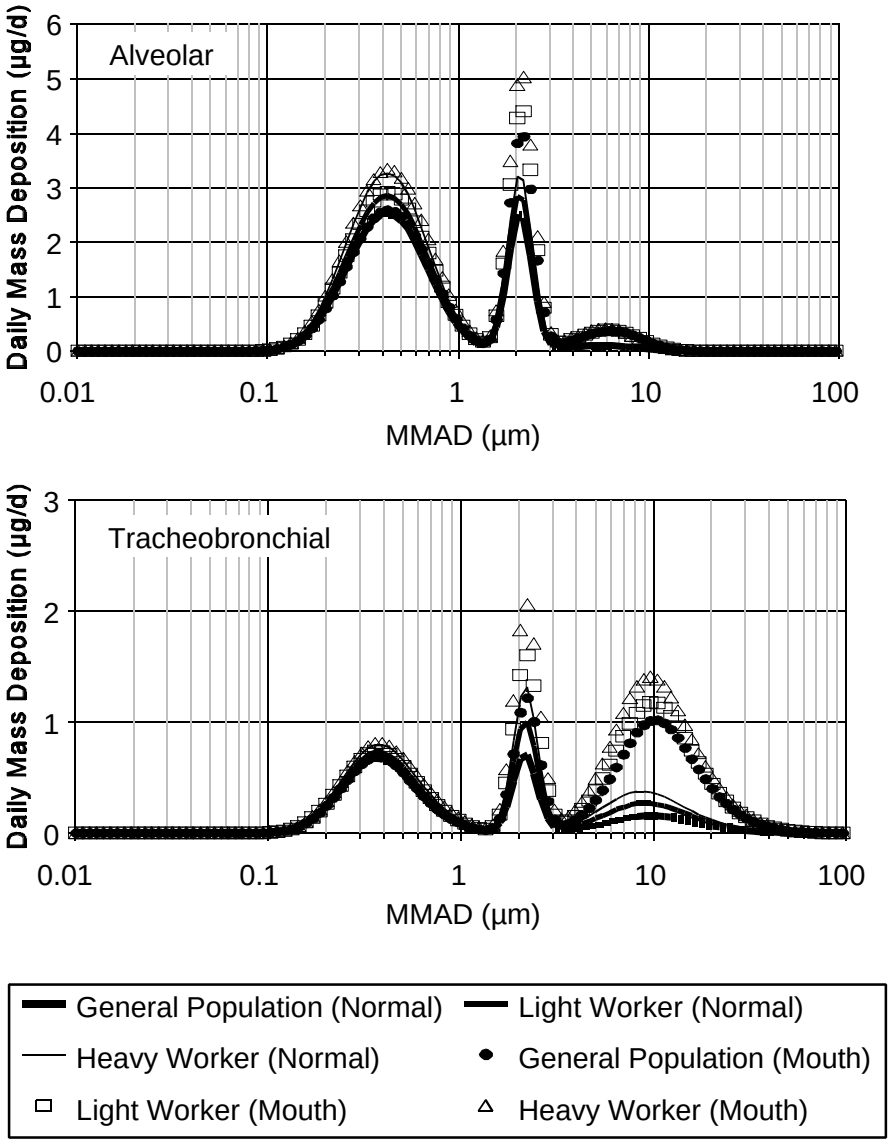

Figure 10-40. Daily mass deposition (μg/day) in tracheobronchial and alveolar regions for normal augmenter versus mouth breather adult males using International Commission on Radiological Protection Publication 66 (ICRP66) (1994) minute volume activity patterns (general population; worker-light activity; worker-heavy activity). The 1994 ICRP66 model simulated an exposure at 50 μg/m^3 to the Philadelphia aerosol described in Appendix 10C.

of the three chosen ambient aerosols. To better understand the deposition differences for each mode, however, the previous Tables 10-19 through 10-24 should also be consulted.

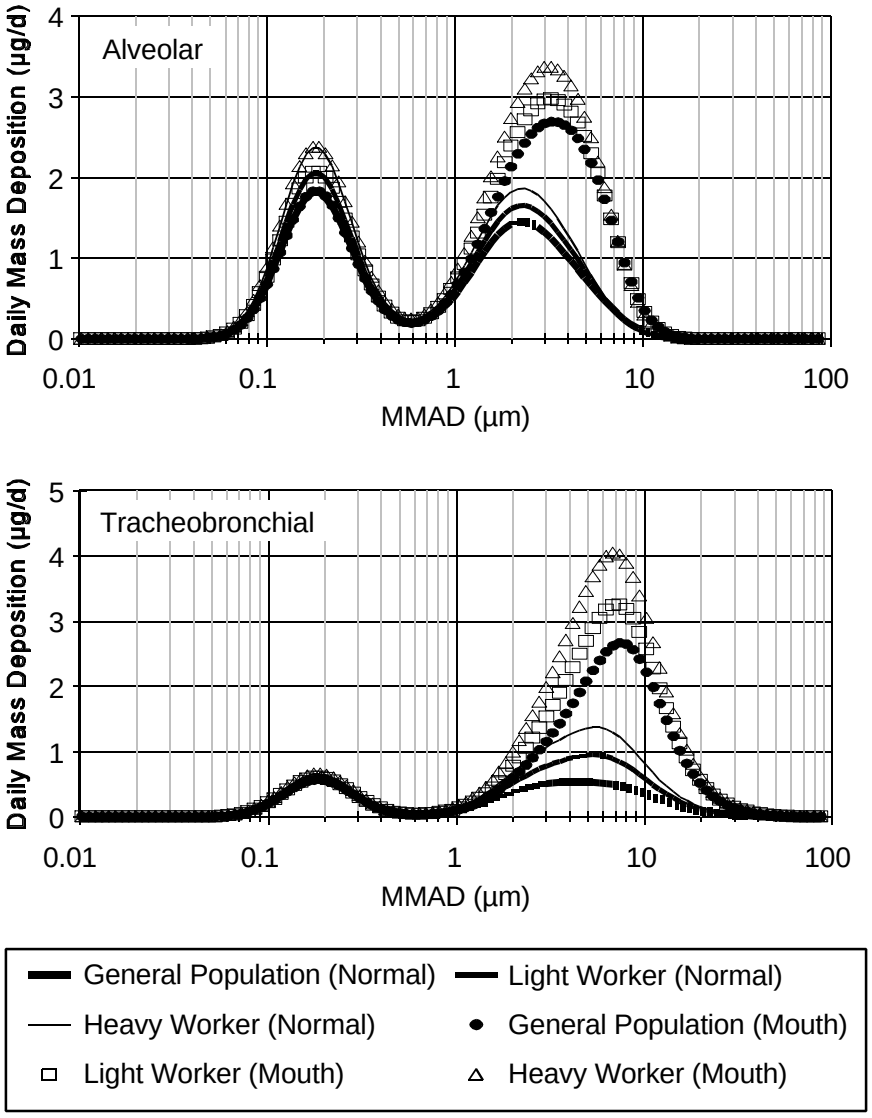

Figure 10-41. Daily mass deposition (μg/day) in tracheobronchial and alveolar regions for normal augmenter versus mouth breather adult males using International Commission on Radiological Protection Publication 66 (ICRP66) (1994) minute volume activity patterns (general population; worker-light activity; worker-heavy activity). The 1994 ICRP66 model simulated an exposure at 50 μg/m^3 to the Phoenix aerosol described in Appendix 10C.

Intraspecies Variability

The different deposition predictions for normal augmenter versus mouth breathing humans illustrates the variability that differences in ventilation rate introduces to deposition estimates. As discussed in Section 10.4.1.6., age, gender, and disease status can influence

TABLE 10-25. DAILY MASS DEPOSITION OF AEROSOL PARTICLES IN THE RESPIRATORY TRACTS OF "NORMAL AUGMENTER" AND "MOUTH BREATHER" ADULT MALE HUMANS EXPOSED TO 50 μg PARTICLES/m^3

Aerosol Figure		10C-1		10C-2(a) (Philadelphia)		10C-2(b) (Phoenix)	
Activity Pattern	Region of Respiratory Tract	Normal Augmenter	Mouth Breather	Normal Augmenter	Mouth Breather	Normal Augmenter	Mouth Breather
		Mass of Particle (μg)					
General population[a]	ET_1	179	80	168	78	235	110
	ET_2	207	178	179	198	260	274
	BB	15	48	6	16	9	37
	bb	42	56	10	12	14	24
	AI	136	175	49	62	55	84
	Total	577	537	411	366	572	528
Workers, light work[b]	ET_1	194	87	182	83	254	118
	ET_2	240	210	214	234	307	325
	BB	24	61	8	20	16	47
	bb	46	61	10	14	14	25
	AI	157	197	56	68	62	91
	Total	661	618	470	419	655	607
Workers, heavy work[c]	ET_1	137	96	206	91	286	129
	ET_2	290	251	258	282	369	390
	BB	86	78	12	25	24	61
	bb	57	68	11	15	17	28
	AI	188	228	63	78	70	103
	Total	760	722	550	490	766	710

[a]Average for 24 h, as derived from ICRP-66 (1994): for 33.3% sleep, 33.3% sitting, and 33.3% light exercise. (See Table 10B-1).
[b]Average for 24 h, as derived from ICRP-66 (1974): for 33.3% sleep, 27.1% sitting, 35.4% light exercise, 4.2% heavy exercise. (See Table 10B-1).
[c]Average for 24 h, as derived from ICRP-66 (1994): for 33.3% sleep, 16.7% sitting, 41.7% light exercise, 8.3% heavy exercise. (See Table 10B-1).

deposition in the respiratory tract. Because the simulations in the preceding section were performed with parameters for adult males using an activity pattern for the general population, an effort to develop activity patterns for different demographic groups was undertaken.

Previous efforts on establishing and revising the NAAQS for ozone and carbon monoxide have attempted to simulate the movement of people through zones of varying air quality so as to approximate the actual exposure patterns of people living within a defined area (Johnson et al., 1989; 1990; 1995a,b). The approach has been implemented through an evolving methodology referred to as the NAAQS exposure model (NEM). The NEM includes data on ventilation rates for various cohort populations.

These cohort data were analyzed to create daily ventilation breathing pattern data for eight demographic groups as follows:

1. Adult Male (18 to 44 years)
2. Adult Female (18 to 44 years)
3. Elderly Male (over 65 years)
4. Elderly Female (over 65 years)
5. Children (0 to 5 years)
6. Children (6 to 13 years)
7. Children (14 to 18 years)
8. Compromised

The compromised demographic group was limited to adults 19 years of age. The objective of identifying this cohort was to construct an activity pattern for subjects with symptoms consistent with cardiopulmonary disease. Those who met this age criterion were included if they answered "yes - it limits my activity" to one of the following questions from a study of the activity patterns affecting exposure to air pollution (Johnson, 1989):

1. Has a doctor ever determined that you have asthma?
2. Has a doctor ever determined that you have a heart condition?
3. Has a doctor ever determined that you have angina?
4. Have you had a stroke?
5. Have you ever had a heart attack?

6. Has a doctor ever determined that you have hypertension (high blood pressure)?

7. Has a doctor ever determined that you have chronic bronchitis?

8. Do you have any other diagnosed respiratory or heart ailment which limits your activity?

Respondents were also included if they answered "yes - it does not limit my activity" to question numbers 1, 2, 3, 4, 5, or 7.

Figures 10B-1 through 10B-3 in Appendix 10B show the daily minute volume patterns for each of these demographic groups. The average minute volume for each of 4 time periods: (1) 24:00 to 06:00; (2) 06:00 to 12:00; (3) 12:00 to 21:00; and (4) 21:00 to 24:00 was used as input to the 1994 ICRP model in order to create a total 24-h daily breathing pattern for each demographic group.

Figure 10-42 shows the fractional deposition in each of the three respiratory tract regions for these demographic groups. Figure 10-43 shows the daily deposition rate (μg/day) of an exposure to 50 $\mu g/m^3$. Some variation between the cohorts exists in the mass deposition fraction for particles in the aerodynamic size range of the ET region; the cohorts of children, especially the 0 to 5 year age group, show an increased deposition. In the A region, the cohort of children 14 to 18 years showed an enhanced deposition rate (μg/d) for submicron-sized of particles in all three regions of the respiratory tract, whereas the cohort of children 0 to 5 years showed a decreased deposition rate relative to male and female adults. For larger particles (micron-sized and above), the 14 to 18 year cohort showed no enhanced deposition rate in the tracheo bronchichial or alveolar regions compared to adults, and younger children cohorts showed a progressive decrease with decreasing age. When evaluated on the basis of daily mass deposition rate (μg/d), the cohort of children ages 14 to 18 years showed an increase in deposition for all three regions of the respiratory tract (Figure 10-43) compared to other cohorts, whereas the cohort of children 0 to 5 years showed a decrease. This is due primarily to differences in respiratory frequency.

Although constructed for differences in age, gender, and health status, the cohorts as constructed represent differences for these factors only characterized in terms of differences in hourly minute volume patterns. Other effects on dosimetry such as altered respiratory tract architecture leading to altered flow pattern or differences in susceptibility of the target

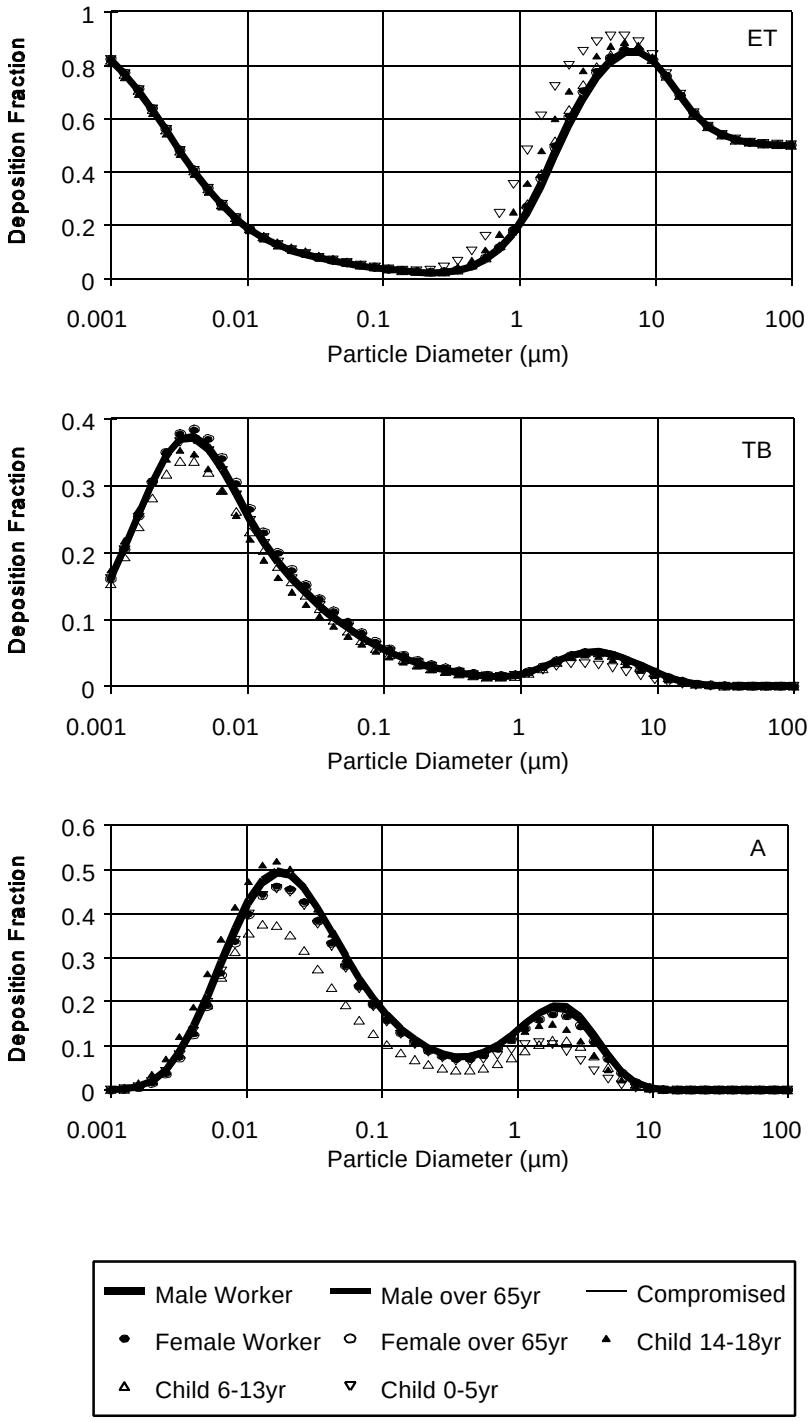

Figure 10-42. Deposition fraction in each respiratory tract region as predicted by the International Commission on Radiological Protection Publication 66 (ICRP66) (1994) model. Simulations used daily minute volume activity patterns for different demographic groups as provided in Appendix 10B.

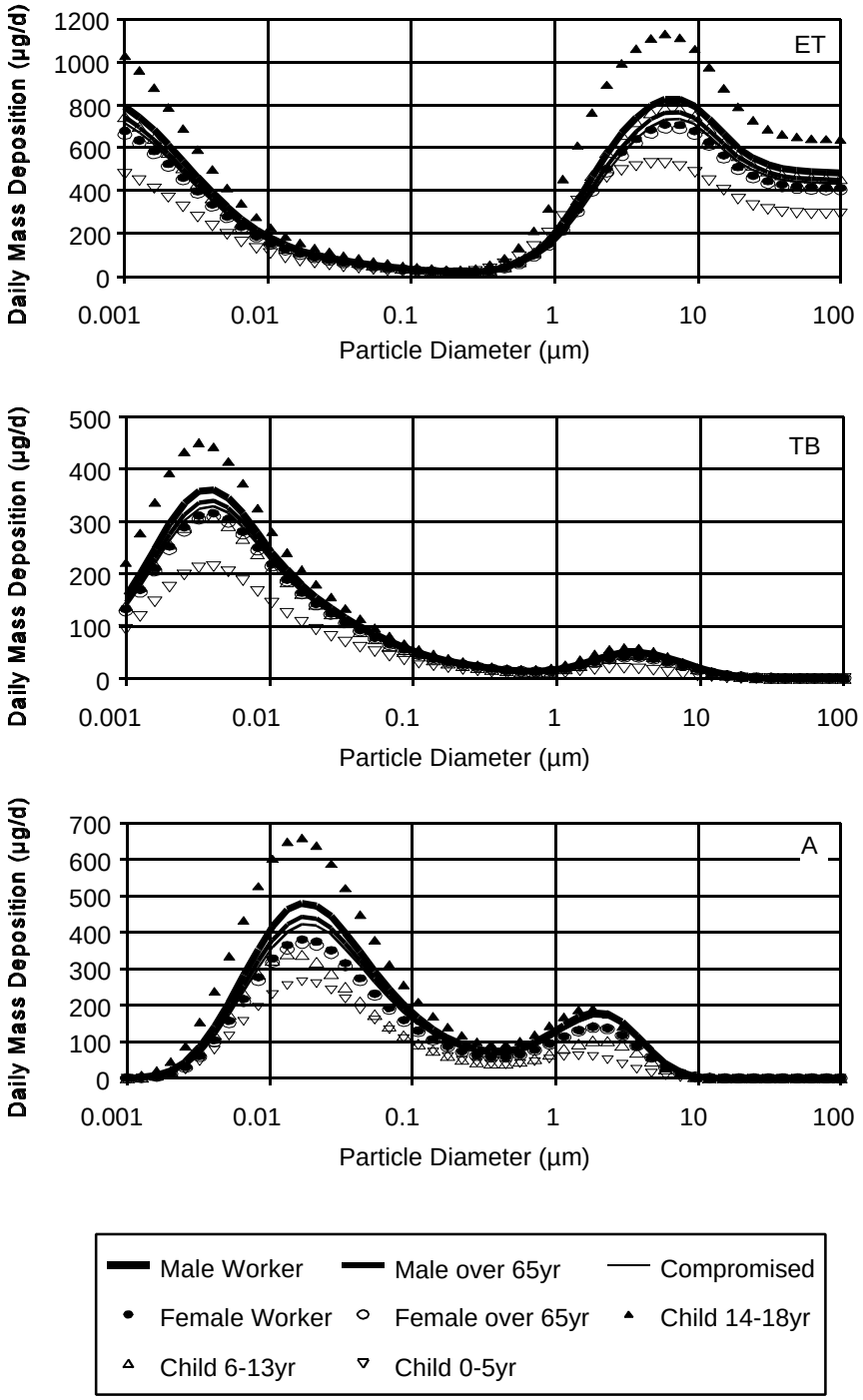

Figure 10-43. Daily mass particle deposition rates (μg/d) for 24-hour exposure at 50 μg/m^3 in each respiratory tract region as predicted by the International Commission on Radiological Protection Publication 66 (ICRP66) (1994) model. Simulations used daily minute volume activity patterns for different demographic groups as provided in Appendix 10B.

tissue are not addressed in these simulations. As discussed earlier, Anderson et al. (1990) have shown enhanced deposition in patients with COPD compared to healthy subjects. Miller et al. (1995) used a more detailed theoretical multipath model and estimated enhanced deposition in a compromised lung status model defined by decreased ventilation to respiratory tract region adjustment. The simulations performed herein were limited to average mass particle burdens per region of the respiratory tract. Nevertheless, these simulations do suggest differences for these cohorts. For example, the cohort for children 14 to 18 years showed an enhanced deposition rate (ug/d) in all three respiratory tract regions whereas children 0 to 5 years showed a decrease.

Relevance to PM_{10} Versus $PM_{2.5}$ Sampling

The dosimetry of particles of different sizes in the human respiratory tract formed one of the primary bases for selecting the PM_{10} size fraction in the 1987 review. Particles in this size range pose the greatest risk to human health because they penetrate to the putative target regions in the lower respiratory tract associated with mortality and morbidity, i.e., the TB and A regions.

Ambient aerosols have been established as bimodal distributions of particles. Fine and coarse particles generally have different sources, formation mechanisms, physical properties, chemical composition and properties, atmospheric lifetimes, and outdoor to indoor infiltration ratios. The fine fraction has been suggested to provide a better exposure surrogate for the epidemiological data (See Chapters 12 and 13). In addition, some of the properties of fine particles may play a role in possible mechanisms of toxicity. For example, the fine mode accounts for most of the particle number and much of the surface area. Also, several chemical classes of concern such as acids and sulfates are found predominantly in the fine fraction. If particle number and not mass alone is an important determinant of response, then a refined characterization of this mode may enhance the ability to discern effects in the exposed populations.

Simulations were performed using the 1994 ICRP66 dosimetry model to illustrate the relationship between deposition efficiency of the respiratory tract, mass burden of particles in the thoracic portion of the respiratory tract, and the mass distribution of aerosols collected by a PM_{10} or $PM_{2.5}$ sampler.

Figure 10-44 shows the predicted regional deposition fraction in the respiratory tract, relative to unit mass concentration in ambient air, as a function of the aerosol size (represented by the mass median aerodynamic diameter, MMAD, in μm). The top graph is for aerosols with a

geometric standard deviation (σ_g) of 1.8 and the other with a σ_g of 2.4. Deposition fraction based on model simulations are shown for the thoracic region (i.e., tracheobronchial plus alveolar deposition, TB + A), as well as for the total respiratory tract deposition fraction. The difference between total respiratory tract and total thoracic fractions represents the extrathoracic or upper airway deposition fraction. In addition these figures show curves representing the fraction collected by a PM_{10} sampler. This illustrates that the PM_{10} sample accounts for almost all of the thoracic deposition, but does not account for many of the larger particles which would be deposited in the ET region. Two curves for the PM_{10} collection fraction are shown illustrating different wind speed characteristics (i.e., for 2 km/h or 8 km/h). It is seen that wind speed is not a major factor. These curves represent the deposition fractions for healthy people who breathe oronasally during exercise (normal augmenters) and healthy people who breathe predominantly through their mouth (mouth breather). As before, it is clear that mouth breathers have a greater deposition of particles >1 μm than do oronasal breathers.

Figures 10-45 and 10-46 expand on the information presented in 10-44 by illustrating deposition fraction in each of the two thoracic regions, the alveolar and the TB region, again for normal augmenters and for mouth breathers. In addition, the collection fraction for a $PM_{2.5}$ sampler is illustrated. Whereas PM_{10} accounts for all particles in the thoracic size deposition mode, the $PM_{2.5}$ sample does not include some larger particles that would be deposited in the TB and A regions of mouth breathers, under the simulated conditions (general population activity pattern 8 h sleep, 8 h sitting, 8 h light activity [see Appendix 10B, Table 10B-1(b)]. Mouth breathers do not represent a large percentage of the population, but are cited here to illustrate the effect of breathing habit. Figure 10-46 provides the same information as Figure 10-45 but expands the scale for micron-sized particles by excluding particles smaller than 0.1 μm.

These simulations (Figures 10-44 through 10-46) represent single mode aerosols of various MMAD and two different σ_g. However, the real world ambient aerosols are

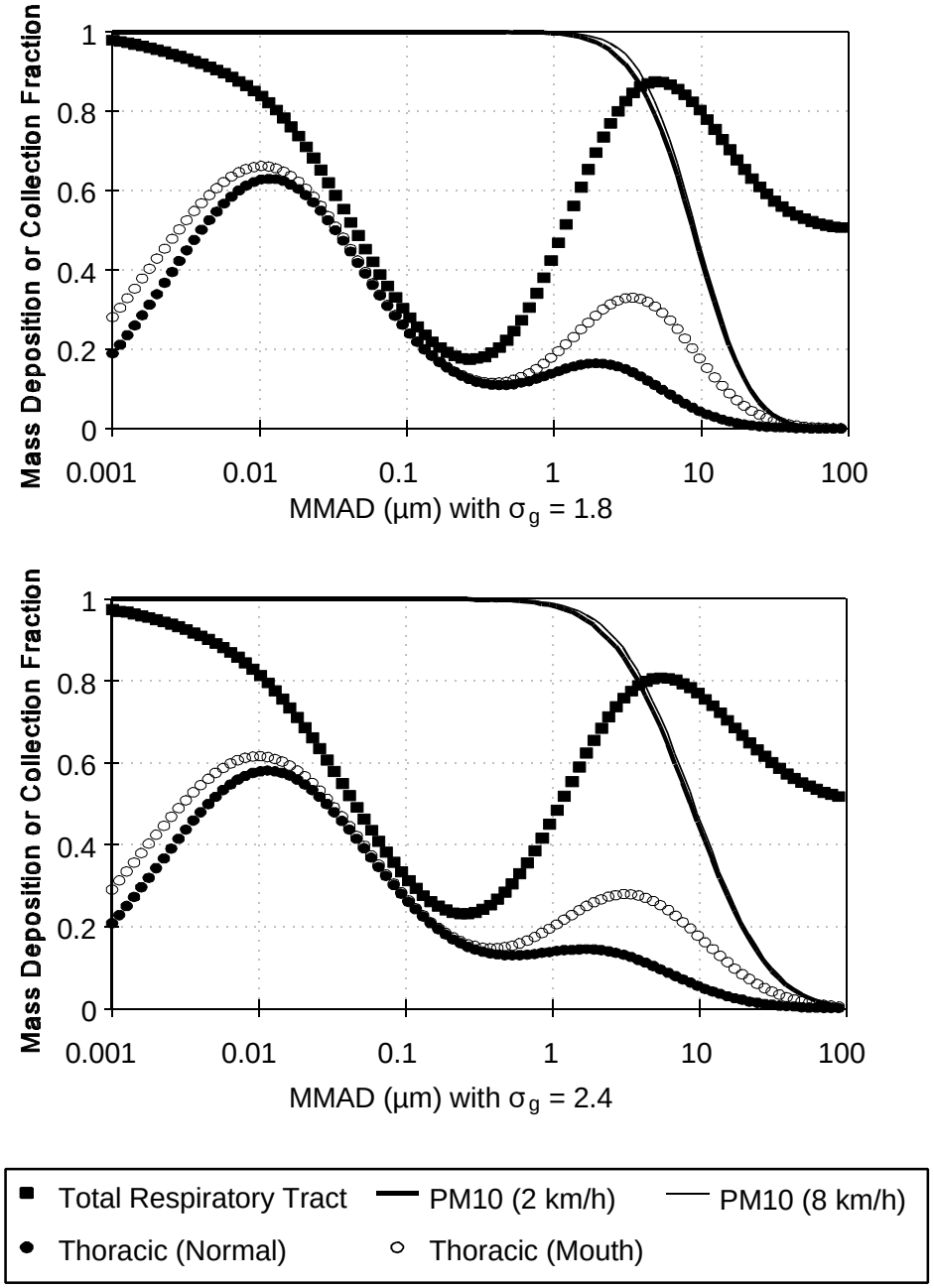

Figure 10-44. Respiratory tract deposition fractions and PM_{10} sampler collection versus mass median aerodynamic diameter (MMAD) with two different geometric standard deviations (σ_g = 1.8 or σ_g = 2.4). Thoracic deposition fraction predicted for normal augmenter versus mouth breather adult male using a general population (ICRP66) minute volume activity pattern and the 1994 ICRP66 model. Total respiratory tract deposition fraction also shown for normal augmenter. PM_{10} sampler collection shown at two different wind speeds (8 km/h or 2 km/h).

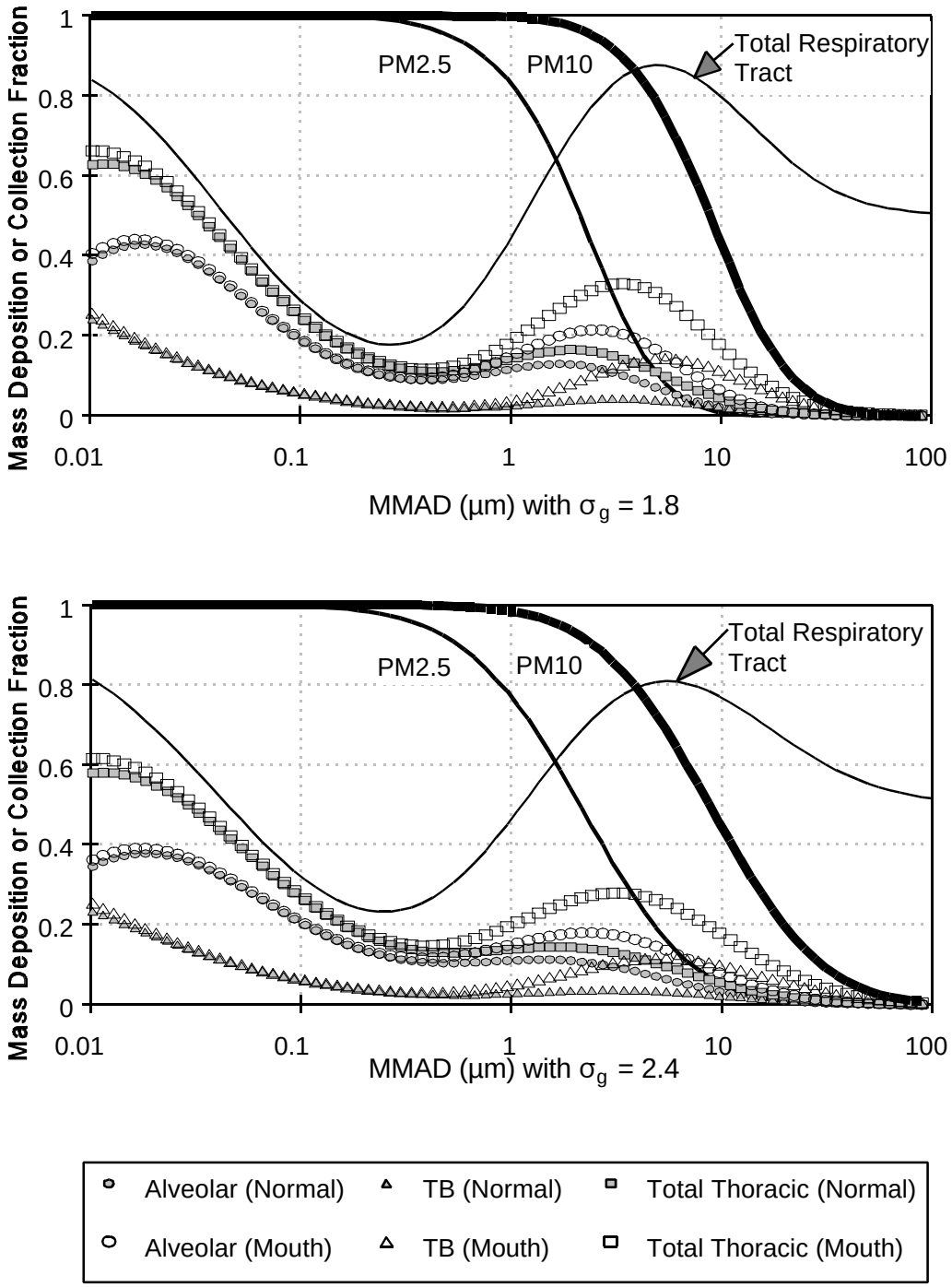

Figure 10-45. Respiratory tract deposition fractions and PM_{10} or $PM_{2.5}$ sampler collection versus mass median aerodynamic diameter (MMAD) with two different geometric standard deviations (σ_g = 1.8 or σ_g = 2.4). Alveolar, tracheobronchial, or total thoracic deposition fractions predicted for normal augmenter versus mouth breather adult male using a general population (ICRP66) minute volume activity pattern and the 1994 ICRP66 model.

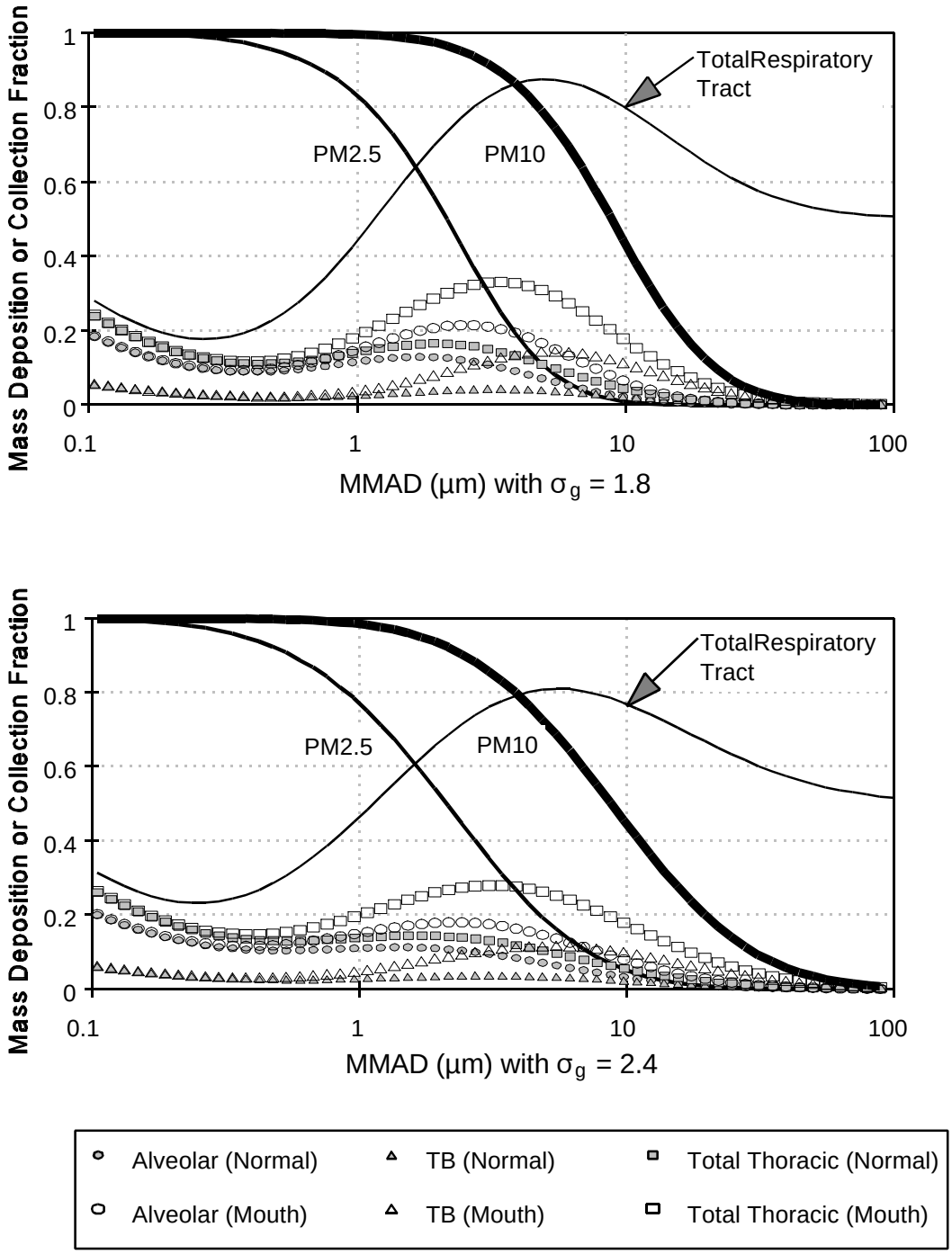

Figure 10-46. Respiratory tract deposition fractions and PM_{10} or $PM_{2.5}$ sampler collection fractions versus mass median aerodynamic diameter (MMAD) with two different geometric standard deviations (σ_g = 1.8 or σ_g = 2.4). Alveolar, tracheobronchial, or total thoracic deposition fractions predicted for normal augmenter versus mouth breather adult male using a general population (ICRP66) minute volume activity pattern and the 1994 ICRP66 model.

multi-modal, having a broad distribution of particle sizes and composition. Figure 10-47 illustrates graphically the process of taking the mass distribution for an ambient aerosol and the deposition efficiency curve for a "typical" (general population adult male) human and deriving the distribution of particle mass deposited in the lung. This is shown in the sequence of graphs in Figure 10-47. The mass distribution of the ambient aerosol (Figure 10-47a) is combined with the deposition efficiency curve (Figure 10-47b; similar to Figure 10-39) to obtain the thoracic mass deposition for the ambient aerosol (Figure 10-47c). The corresponding process for collection with a PM_{10} sampler is also shown. Figure 10-47a (ambient mass distribution) is combined with the sampler efficiency curve (Figure 10-47d), resulting in Figure 10-47e, which shows the collected mass distribution for the ambient aerosol. If Figure 10-47c is superimposed on Figure 10-47e, figures such as 10-48 and 10-49 will be generated.

Figures 10-48 and 10-49 illustrate the fractional mass deposition seen with representative ambient aerosols for the cities of Phoenix and Philadelphia. These trimodal aerosols were described in Chapter 3, and their parameters are provided in Appendix 10C. From these graphs it is shown that the $PM_{2.5}$ sampler distribution accounts for the particle mass in the fine (<1.0 μm) mode and the transition mode (MMAD ~2.5 μm) but does not account for the smaller mass of coarse mode particles that would be deposited in the thorax (mainly affecting tracheobronchial deposition in mouth breathers). Failure of the $PM_{2.5}$ sampler to account for coarse mode particle thoracic deposition is more evident for the Phoenix aerosol than for the Philadelphia aerosol.

Because mass deposition is not the only dose metric that is of interest, a similar modeling exercise was conducted for particle number, using the Philadelphia and Phoenix aerosols. Simulations were again performed with parameters for adult males and a general population activity pattern. Figure 10-50 shows the predicted fraction of total number of particles inhaled that is deposited in each region of the respiratory tract (ET, TB, A) for the Philadelphia aerosol. Figure 10-51 shows the number of particles deposited each day in each respiratory tract region for the Philadelphia aerosol assuming an exposure to a total particulate mass concentration of 50 $\mu g/m^3$. These figures show that a large fraction of the number of deposited particles is contributed, as anticipated, by the fine fraction mode, and that this can represent a very large number of particles deposited per day (on the order of

Figure 10-47. Schematic illustration of how ambient aerosol distribution data were integrated with respiratory tract deposition efficiency (using 1994 ICRP66 model) or sampler efficiency to calculate deposition in respiratory tract regions or mass collected by sampler.

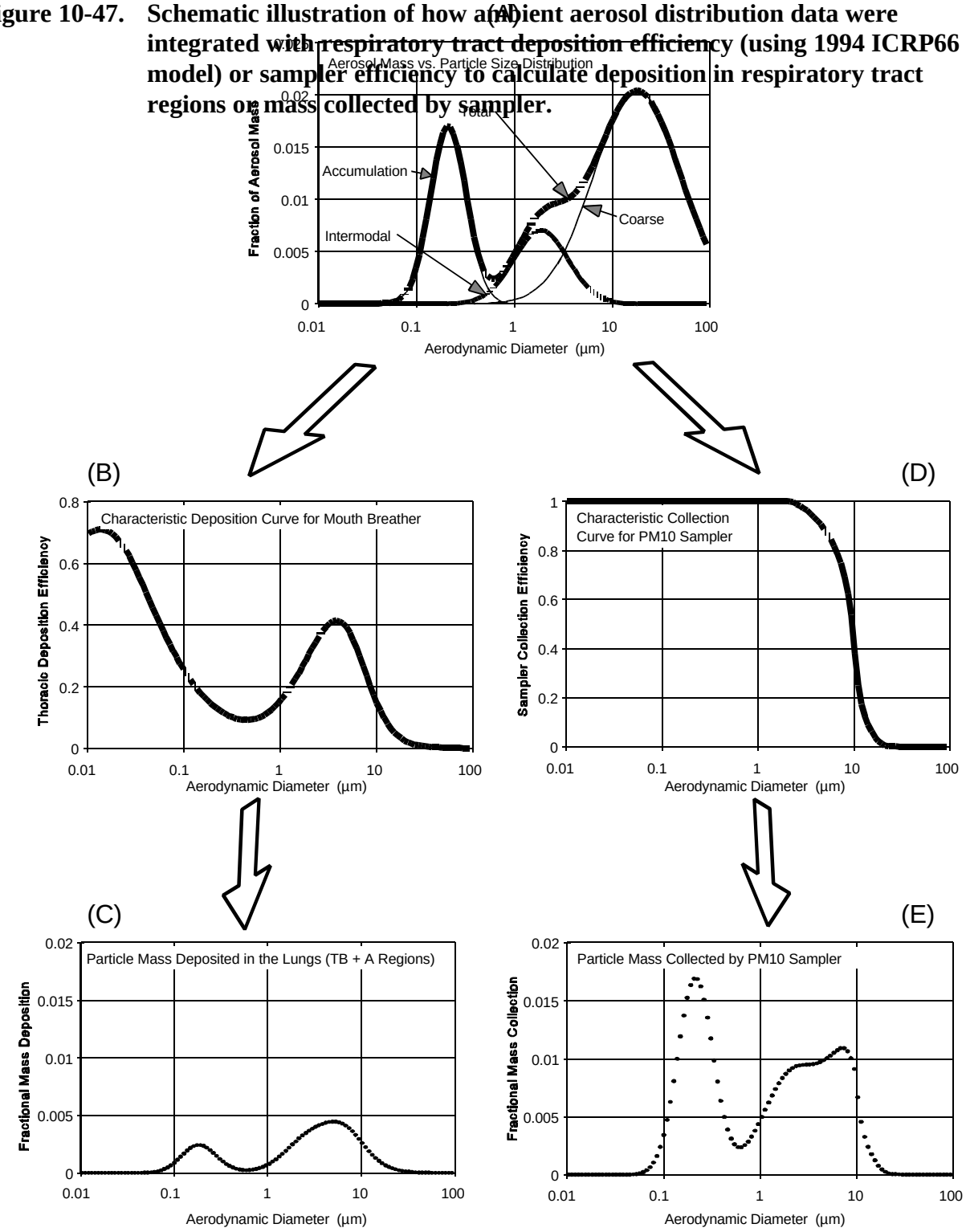

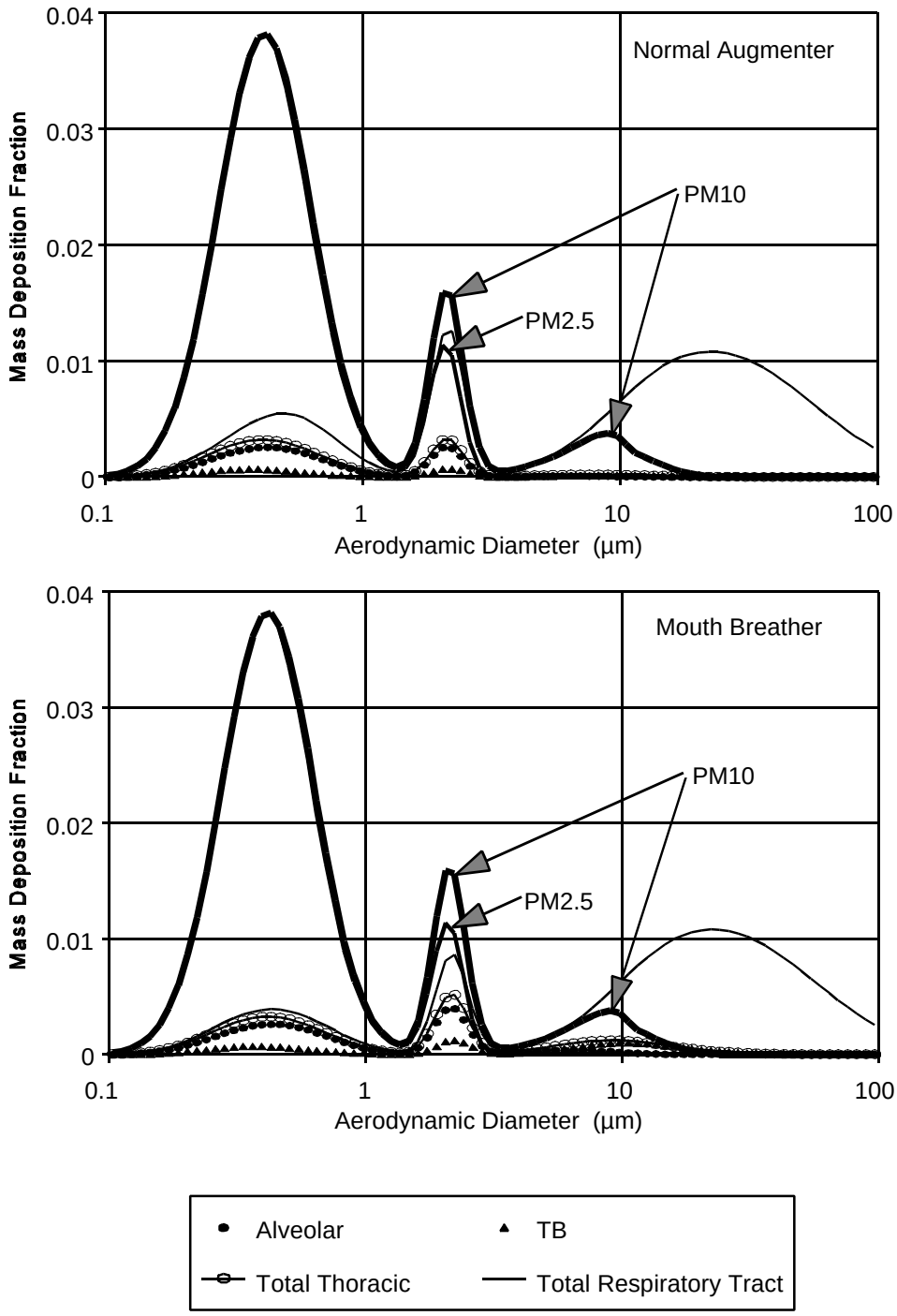

Figure 10-48. Mass deposition fraction in normal augmenter versus mouth breather adult male with a general population minute volume activity pattern predicted by the International Commission on Radiological Protection Publication 66 (1994) model and the mass collected by PM_{10} or $PM_{2.5}$ samplers for Philadelphia aerosol (described in Appendix 10C).

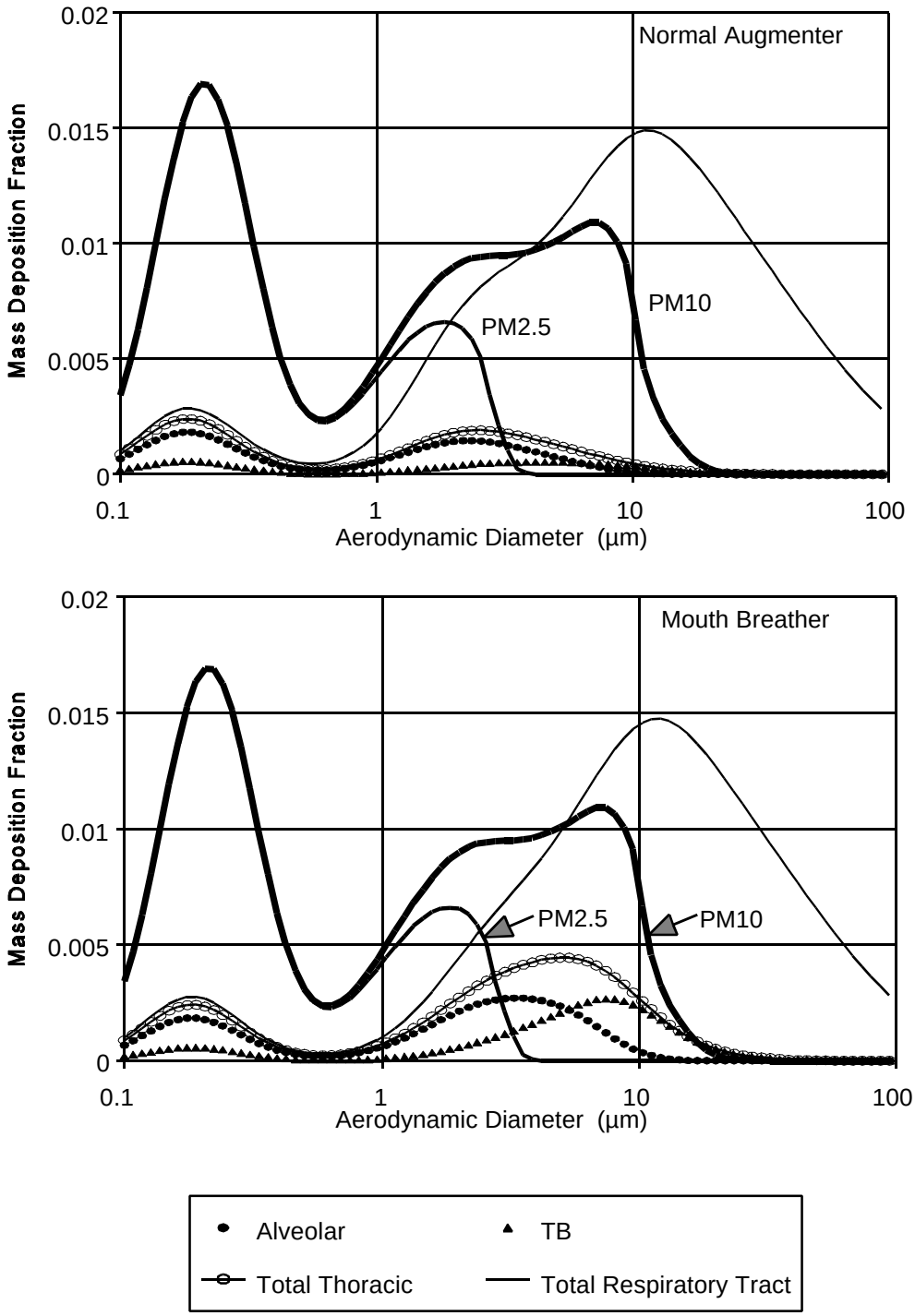

Figure 10-49. Mass deposition fraction in normal augmenter versus mouth breather adult male with a general population minute volume activity pattern predicted by the International Commission on Radiological Protection Publication 66 (1994) model and the mass collected by PM_{10} or $PM_{2.5}$ samplers for Phoenix aerosol (described in Appendix 10C).

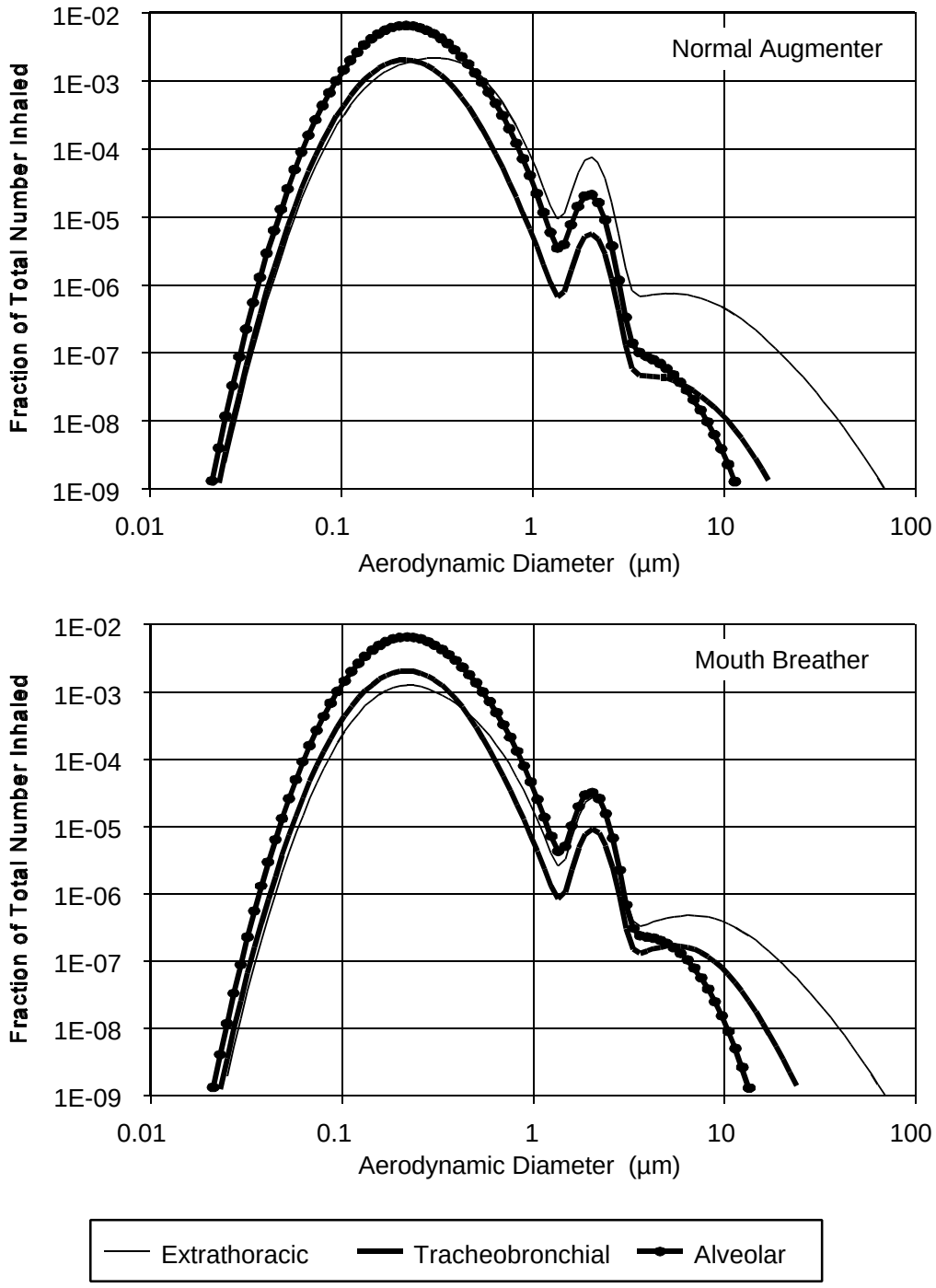

Figure 10-50. Fractional number deposition in each respiratory tract region for normal augmenter versus mouth breather adult male with a general population activity pattern as predicted by the International Commission on Radiological Protection Publication 66 (1994) model for an exposure to the Philadelphia aerosol (described in Appendix 10C).

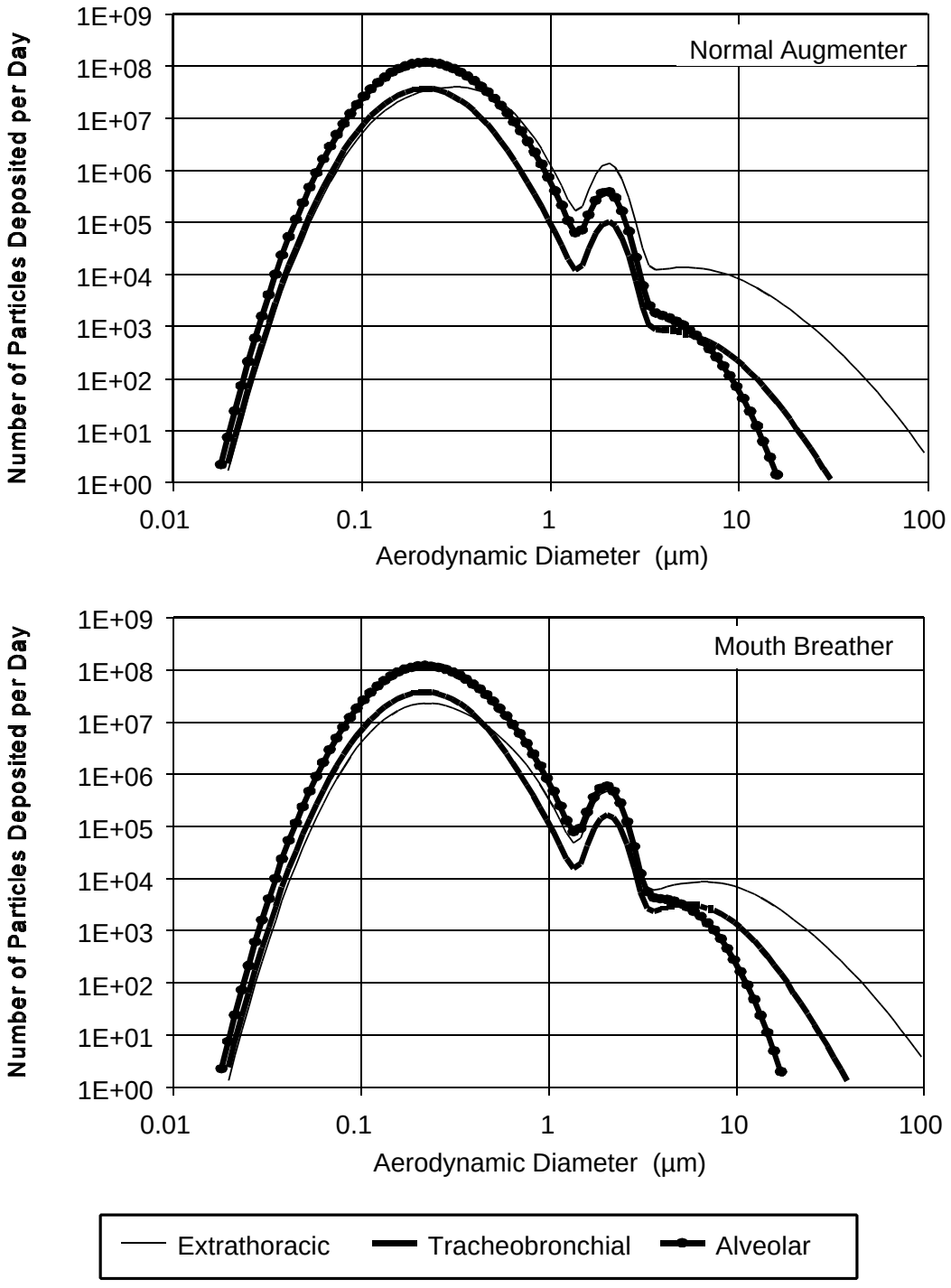

Figure 10-51. Number of particles deposited per day in each respiratory tract region for normal augmenter versus mouth breather adult male with a general population activity pattern as predicted by the International Commission on Radiological Protection Publication 66 (1994) model for an exposure to the Philadelphia aerosol (described in Appendix 10C) at a concentration of 50 μg/m^3.

100,000,000) in the alveolar region. Figure 10-52 shows the predicted fraction of total number of particles inhaled that is deposited in each respiratory tract region for the Phoenix aerosol, and Figure 10-53 shows the number of particles deposited each day in each respiratory tract region for this aerosol assuming an exposure to a total particulate mass concentration of 50 μg/m^3. The more disperse intermodal fraction of the Phoenix aerosol (see Figure 10C-2 in Appendix 10C) contributes more particles to the fine mode size-range than that of the Philadelphia aerosol.

Hygroscopic Aerosols

The ICRP66 (1994) deposition model as so far described relates to the distribution of activity or mass of aerosol particles with respect to their size on entering the respiratory tract. However, in the case of a hygroscopic material, it is necessary to take account of the increase in particle size that occurs when such materials are exposed to the near-saturated air in the respiratory tract. The ICRP66 model can be applied for hygroscopic materials by replacing the values of particle aerodynamic diameter, d_{ae}, and diffusion coefficient, D, in ambient air with the values $d_{ae}(j)$ and D_j attained in each region, j, of the respiratory tract.

Annexe D of ICRP66 describes how the growth of a hygroscopic particle can be approximated in general terms as a function of its residence time in saturated air at body temperature. For a residence time, t_j^r, in region, j, measured from inspiration of the particle (*i.e.*, entry to the nose or mouth), the particle aerodynamic diameter and diffusion coefficient attained by hygroscopic growth are approximately related to $d_{ae}(0)$ and D(0), the respective values in ambient air (*i.e.*, the external environment), and the values at equilibrium, $d_{ae}(\ )$ and D(\ ) are

$$d_{ae}(t_j^r) = d_{ae}(\ ) - [d_{ae}(\ ) - d_{ae}(0)] \exp\left[-\{10\, t_j^r\}^{0.55} \left[\frac{D(0)}{d_{ae}(0)}\right]\right]^{0.6}, \text{ and} \qquad (10\text{-}58)$$

$$D(t_j^r) = D(\ ) + [D(0) - D(\ )] \exp\left[-\{10\, t_j^r\}^{0.55} \left[\frac{D(0)}{d_{ae}(0)}\right]\right]^{0.6}.$$

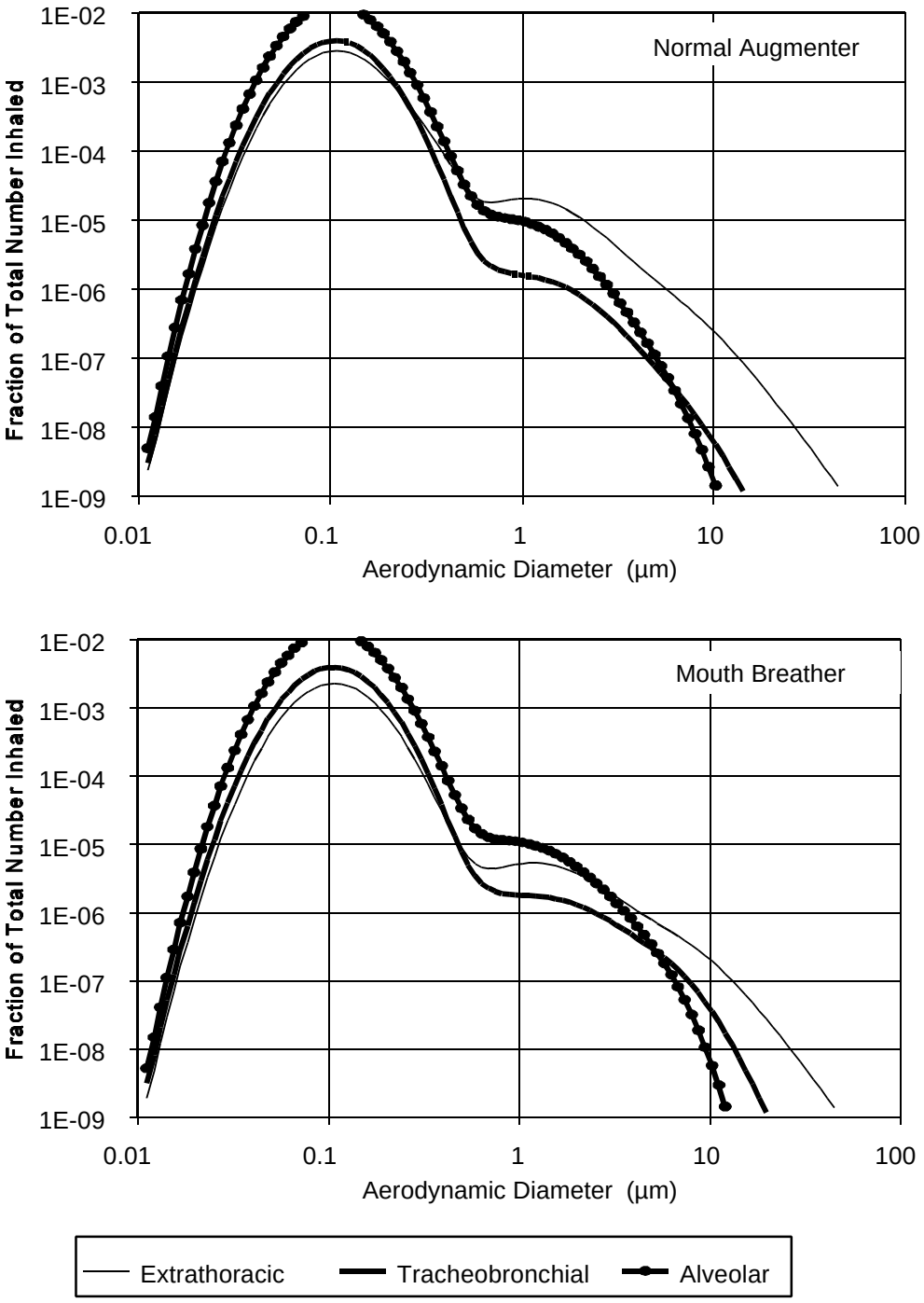

Figure 10-52. Fractional number deposition in normal augmenter versus mouth breather adult male with a general population activity pattern predicted by the International Commission on Radiological Protection Publication 66 (1994) model for an exposure to the Phoenix aerosol (described in Appendix 10C).

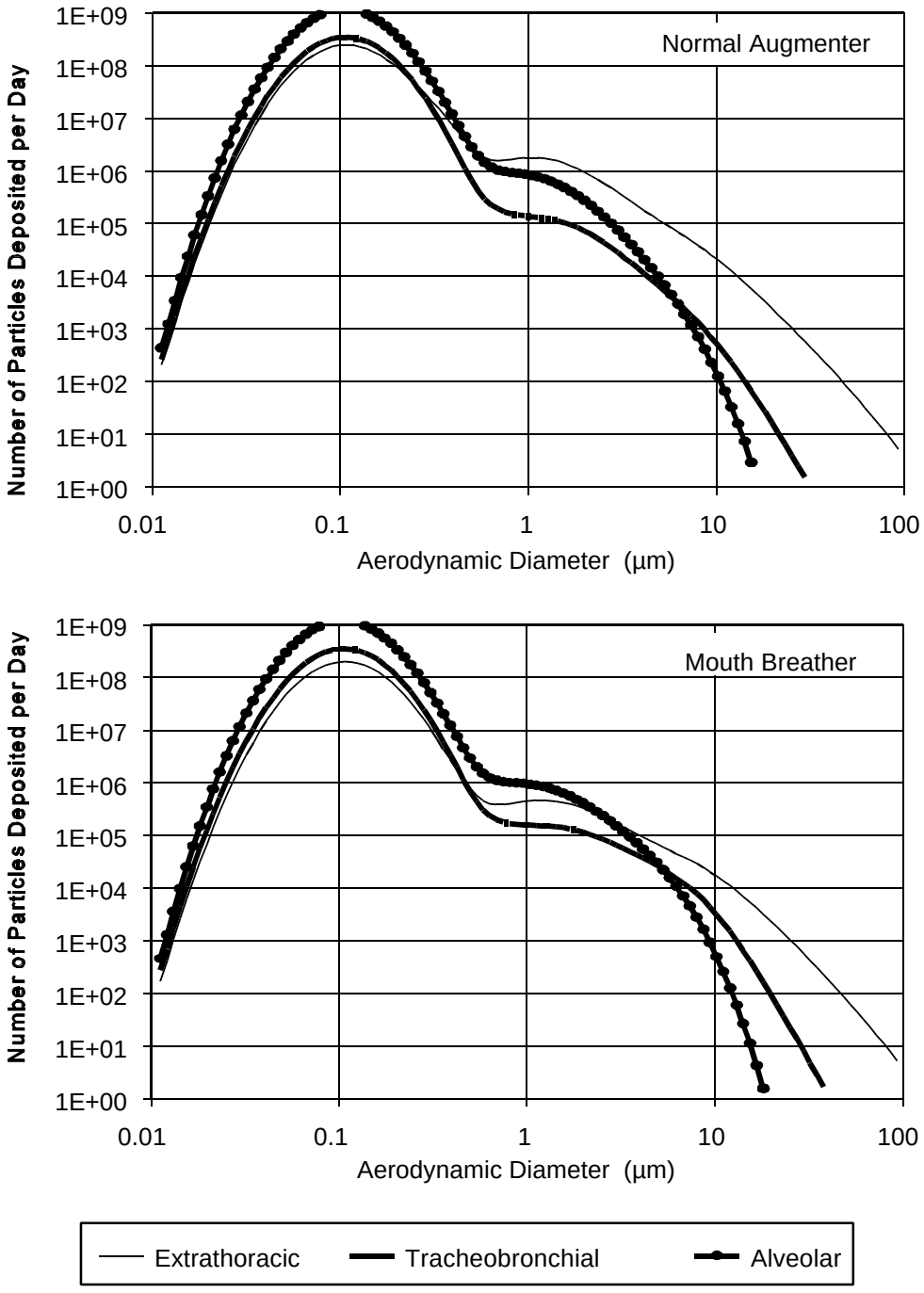

Figure 10-53. Number of particles deposited per day in each respiratory tract region for normal augmenter versus mouth breather adult male with a general population activity pattern predicted by the International Commission on Radiological Protection Publication 66 (1994) model for an exposure to the Phoenix aerosol (described in Appendix 10C) at a concentration of 50 μg/m^3.

To solve the model for a specific material, it is necessary to specify the degree of particle size growth at equilibrium. This generally lies in the range of two- to fourfold growth, depending on the amount of hygroscopic material associated with the particle. However, ICRP66 suggests that it is likely to be adequate to assume by default a threefold growth factor at equilibrium, for substitution in these equations. Note that the initial aerodynamic diameter, $d_{ae}(0)$, is increased by particle growth, whereas the initial diffusion coefficient, D(0), is decreased.

The effect of hygroscopic particle growth is generally to decrease total lung deposition for submicron-sized particles, and to increase it for larger particles. As discussed in some detail in Annexe D of ICRP66, the particle size in ambient air corresponding to minimum lung deposition is reduced from about 0.4 μm for non-hygroscopic particles to about 0.1 μm for hygroscopic particles (Tu and Knutson, 1984; Blanchard and Willeke, 1984).

Intrahuman Variability in Regional Deposition

The experimental data on regional deposition of particles in the human respiratory tract indicate substantial intersubject variability, even if the particles are inhaled under identical exposure conditions. In ICRP66, the upper and lower 95% confidence bounds of the data are represented by a variable coefficient, a, which is incorporated into each algebraic expression for deposition efficiency (see ICRP66, Chapter 5, Tables 12 and 13, pp. 45 and 46). In each case, the coefficient is taken to be log-normally distributed, (i.e., $a_{upper} = a_{median} \times \sigma_g^2$, and $a_{lower} = a_{median} \div \sigma_g^2$) where σ_g is the fitted geometric standard deviation. Other confidence bounds on the predicted regional deposition efficiency are given by substituting an appropriate value of the coefficient, a, that is sampled from the defined log-normal distribution.

Representing the median (or expectation) value of the coefficient, a, for each region, j, by a_j, then it is convenient to use a dimensionless scaling constant, c_j, as a multiplier or divisor of the median value. In Table 14 of ICRP66 (Chapter 5, p. 49), the ICRP gives values of this scaling constant that are estimated to describe the spread in the experimental data for regional respiratory tract deposition. The scaling factors defining the upper and lower 95% confidence bounds of regional deposition range from × or ÷ by 1.4 in the expression for "thermodynamic" deposition efficiency of the extrathoracic (ET) region, to × or ÷ by 3.3 for the "aerodynamic" deposition efficiency of the ET region. To evaluate the uncertainty distribution of the predicted deposition

fractions in all five regions of the respiratory tract (i.e., ET_1, ET_2, BB, bb, and AI) it is necessary to select the respective values of c_j at random from their assumed log-normal distributions.

10.7.5.2 Laboratory Animal Estimates

Tables 10-26 through 10-31 provide the deposition fractions of various particle sizes (MMAD) for either a relatively monodisperse (σ_g = 1.3) versus a more polydisperse (σ_g = 2.4) distribution in humans or rats. Deposition fractions of these aerosols for an adult male human normal augmenter and mouth breather with a general population activity pattern were calculated using the ICRP66 model (ICRP66, 1994). The deposition fraction for each respiratory tract region is presented: ET in Tables 10-26 and 10-27; TB in Tables 10-28 and 10-29; and A in Tables 10-30 and 10-31. These regional deposition fractions are shown plotted in Figure 10-54. The left side in each panel represents the deposition fractions for the relatively monodisperse aerosol (σ_g = 1.3) and the right side in each panel represents the more polydisperse aerosol (σ_g = 2.4). Note that the y-axis scale changes from one panel to the other and from panel to panel. As discussed in Section 10.5, polydispersity in the aerodynamic particle size range tends to smear the regional deposition across the range of particles. The interspecies differences in fractional deposition are readily apparent from these figures.

In the TB region, Figure 10-54 illustrates that at the smaller particle diameters (MMAD < 2 μm for σ_g = 1.3) the rats have higher deposition fractions than normal augmenter (nasal breathing) humans. At larger particle diameters (MMAD > 2.5 μm for σ_g = 1.3), rats have very little deposition in the TB or A regions due to the low inhalability of these particles. This may help explain why inhalation exposures of rodents to high concentrations of larger particles have exhibited little effect in some bioassays.

The information in Tables 10-26 through 10-31 and depicted in the panels of Figure 10-54 can be used to calculate the deposition fraction term in Equations 10-50 and 10-54. The average ventilation rates and parameters such as surface area which could be used for normalizing factors for laboratory animals are found in Appendix 10B, Table 10B-2.

TABLE 10-26. EXTRATHORACIC DEPOSITION FRACTIONS OF INHALED MONODISPERSE AEROSOLS (σ_g=1.3) IN RATS AND HUMAN "NORMAL AUGMENTER" AND "MOUTH BREATHER"

MMAD	Normal Augmenter	Mouth Breather	Rat
1	0.273	0.074	0.18
1.5	0.443	0.141	0.55
2	0.566	0.209	0.74
2.5	0.651	0.270	0.77
3	0.711	0.326	0.76
3.5	0.754	0.375	0.73
4	0.785	0.420	0.70

TABLE 10-27. EXTRATHORACIC DEPOSITION FRACTIONS OF INHALED POLYDISPERSE AEROSOLS (σ_g=2.4) IN RATS AND HUMAN "NORMAL AUGMENTER" AND "MOUTH BREATHER"

MMAD	Normal Augmenter	Mouth Breather	Rat
1	0.326	0.126	0.30
1.5	0.442	0.193	0.42
2	0.524	0.250	0.49
2.5	0.582	0.299	0.53
3	0.624	0.340	0.55
3.5	0.655	0.374	0.56
4	0.678	0.404	0.56

TABLE 10-28. TRACHEOBRONCHIAL DEPOSITION FRACTIONS OF INHALED MONODISPERSE AEROSOLS (σ_g=1.3) IN RATS AND HUMAN "NORMAL AUGMENTER" AND "MOUTH BREATHER"

MMAD	Normal Augmenter	Mouth Breather	Rat
1	0.022	0.026	0.10
1.5	0.033	0.048	0.06
2	0.042	0.074	0.03
2.5	0.048	0.101	0.01
3	0.050	0.125	0.005
3.5	0.050	0.144	0.002
4	0.049	0.159	0.001

TABLE 10-29. TRACHEOBRONCHIAL DEPOSITION FRACTIONS OF INHALED POLYDISPERSE AEROSOLS (σ_g=2.4) IN RATS AND HUMAN "NORMAL AUGMENTER" AND "MOUTH BREATHER"

MMAD	Normal Augmenter	Mouth Breather	Rat
1	0.028	0.049	0.06
1.5	0.032	0.068	0.05
2	0.035	0.084	0.04
2.5	0.036	0.096	0.031
3	0.036	0.104	0.025
3.5	0.036	0.110	0.021
4	0.035	0.114	0.017

TABLE 10-30. ALVEOLAR DEPOSITION FRACTIONS OF INHALED MONODISPERSE AEROSOLS (σ_g=1.3) IN RATS AND HUMAN "NORMAL AUGMENTER" AND "MOUTH BREATHER"

MMAD	Normal Augmenter	Mouth Breather	Rat
1	0.119	0.140	0.06
1.5	0.146	0.120	0.10
2	0.150	0.237	0.06
2.5	0.142	0.256	0.02
3	0.126	0.258	0.011
3.5	0.109	0.248	0.005
4	0.092	0.230	0.002

TABLE 10-31. ALVEOLAR DEPOSITION FRACTIONS OF INHALED POLYDISPERSE AEROSOLS (σ_g=2.4) IN RATS AND HUMAN "NORMAL AUGMENTER" AND "MOUTH BREATHER"

MMAD	Normal Augmenter	Mouth Breather	Rat
1	0.111	0.151	0.04
1.5	0.112	0.171	0.04
2	0.109	0.180	0.035
2.5	0.103	0.179	0.031
3	0.096	0.175	0.027
3.5	0.089	0.169	0.023
4	0.082	0.161	0.020

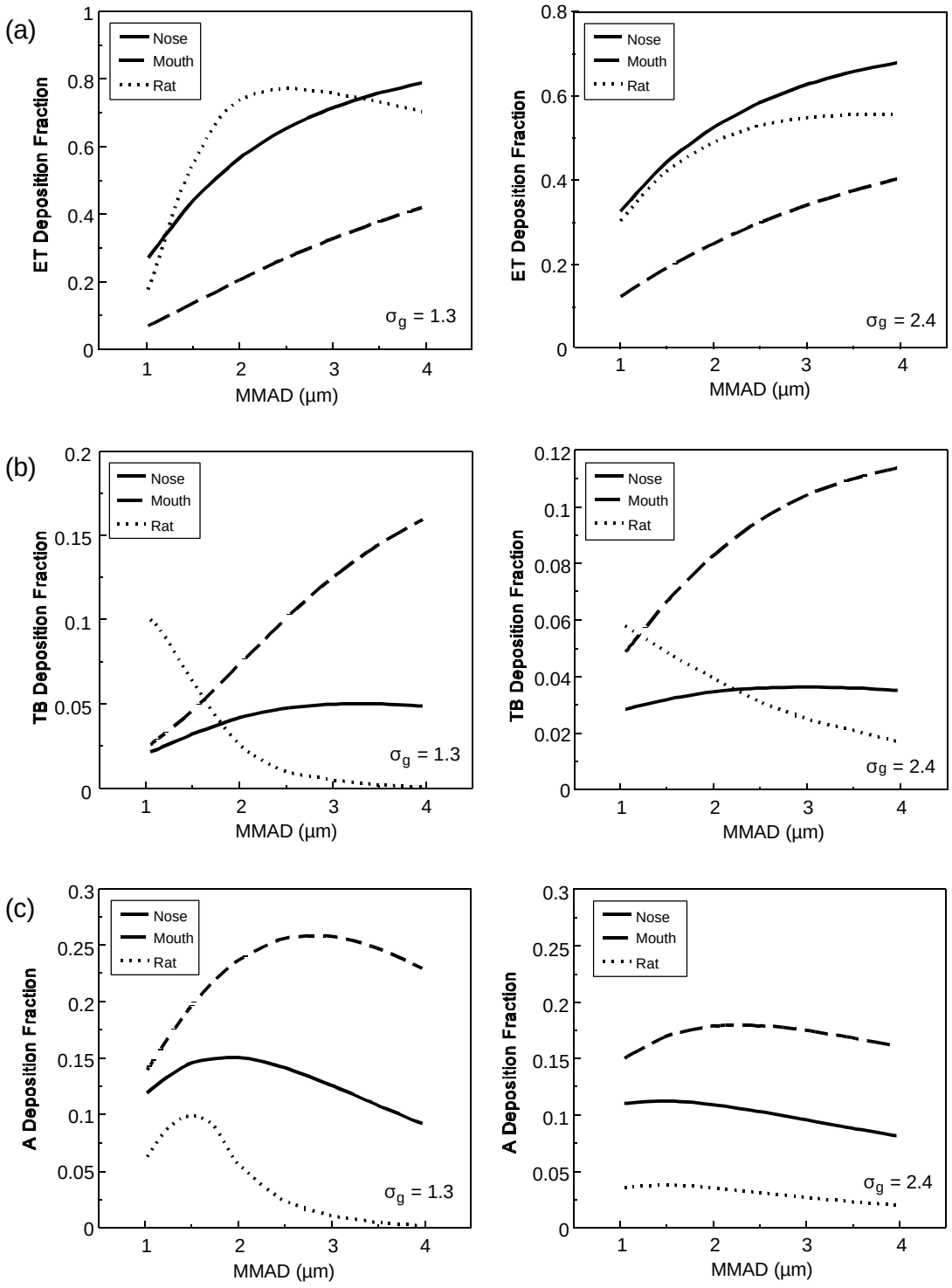

Figure 10-54. Predicted extrathoracic deposition fractions versus mass median aerodynamic diameter (MMAD) of inhaled monodisperse (σ_g = 1.3) aerosols shown in left-side panels or polydisperse (σ_g = 2.4) aerosols shown in right-side panels for humans (nose versus mouth breathing) and rats (obligatory

nose breathers), for (a) the extrathoracic region, (b) tracheobronchial region, and (c) alveolar region.

Respiratory tract region surface areas for humans are found in Table 10B-1. The human male adult general population activity pattern in Table 10B-1 corresponds to a daily ventilation volume of 19.9 m^3/day. This is the average ventilation rate that was used to run the LUDEP® simulations and would be used in the denominator of Equations 10-51 or 10-55. The normal augmenter or mouth breather deposition fractions found in Tables 10-26 through 10-31 represents the sum of the Fr_H factors in the denominator of the expression found in Equations 10-51 and 10-55. Likewise, the deposition fractions for the rat represent the Fr_A factor in Equations 10-53 and 10-57.

Because particles initially deposit along the surface of the respiratory tract, regional surface area is chosen as the normalizing factor for calculation of the regional deposited dose ratio (RDDR), as described in Equation 10-50, in order to characterize "acute" effects. Assuming an exposure to an aerosol with a MMAD of 1.0 μm and σ_g = 1.3, Equation 10-51 can be used to calculate $RDDR_{A[ACT]}$ estimates using the deposition fractions provided in Tables 10-26 through 10-31 and surface area and ventilation rate parameters provided in Tables 10B-1 and 10B-2 in Appendix 10B. A $RDDR_{A[ACT]}$ value of 1.54 is calculated for rats using the alveolar surface area as a normalizing factor. The $RDDR_{A[ACT]}$ value for each species would be applied to an experimental exposure concentration from a laboratory toxicology study using rats to calculate a human equivalent concentration.

Interspecies extrapolation to HEC values allows for comparison among species. For example, if a rat exhibited an effect in the alveolar region when exposed to an aerosol with a MMAD = 1.0 μm and σ_g = 1.3 at an exposure concentration of 100 $\mu g/m^3$, the resultant HEC value calculated for the rat would be 154 $\mu g/m^3$. This HEC would result in a similar alveolar deposited dose and thereby a similar effect in humans, assuming species sensitivity to a given dose is equal. Although laboratory species may be exposed to the same aerosol at the same concentration, each would have a different fractional deposition, which when normalized to regional surface area, could result in different HEC estimates. Thus, taking into account species differences in dosimetry is necessary before comparing effective concentrations when interpreting toxicity data.

For tracheobronchial effects, the $RDDR_{TB[ACT]}$ would be used to adjust exposure concentrations for interspecies differences in dosimetry. For an aerosol with an MMAD = 1.0 μm and σ_g = 1.3, the $RDDR_{TB[ACT]}$ value is 9.95 for rats. For an aerosol with an MMAD = 2.5 and σ_g

= 2.4, the $RDDR_{TB[ACT]}$ value is 1.89. The decrease in the value is due to the decreased inhalability of the larger particle diameter and the effect of polydispersity. Similarly, the $RDDR_{A[ACT]}$ value for an aerosol with an MMAD = 2.5 μm and σ_g = 2.4 is 0.88 for rats, whereas it was 1.54 for the more monodisperse aerosol.

Doses are conventionally expressed in terms of particle mass (gravimetric dose). However, when different types of particles are compared, doses may be more appropriately expressed as particle volume, particle surface area, or numbers of particles, depending on the effect in question (Oberdörster et al., 1994). For example, the retardation of alveolar macrophage-mediated clearance due to particle overload appears to be better correlated with phagocytized particle volume rather than mass (Morrow, 1988). The smaller size fractions of aerosols are associated with the bulk of surface area and particle number. That is, concentrations in this size fraction are very small by mass but extremely high by number. The need to consider alternative dose metrics such as number is accentuated when the high rate of deposition of small particles in the lower respiratory tract (TB and A regions), the putative target for the mortality and morbidity effects of PM exposures, is also taken into account. Simulations of particle number deposition fraction for ambient aerosols characterized for Philadelphia and Phoenix confirm that the fine mode contributes the highest deposition fraction in each region of the respiratory tract. Particle numbers deposited per day were shown to be on the order of 100,000,000 and 1,000,000,000 for the fine mode of Philadelphia and Phoenix, respectively, for hypothetical exposure to a total aerosol mass concentration of 50 $\mu g/m^3$.

Inhalability is a major factor influencing interspecies variability. At the larger particle diameters (MMAD > 2.5 μm for $_g$ = 1.3), the laboratory animal species have very little lower respiratory tract deposition due to the low inhalability of these particles. This may help explain why inhalation exposures of laboratory animals to high concentrations of larger diameter particles have exhibited little effect in some bioassays.

Simulations of retained particle burdens confirmed solubility as a major factor influencing clearance. Assumptions with respect to dissolution-halftimes (10, 100, or 1,000 days) were shown to dramatically influence the predicted particle mass burdens. Data on in vivo solubility are needed to enhance modeling of clearance in all species. Retained particle burden accumulates more rapidly and reaches a higher equilibrium burden when the particles are poorly soluble.

multi-modal, having a broad distribution of particle sizes and composition. Figure 10-47 illustrates graphically the process of taking the mass distribution for an ambient aerosol and the deposition efficiency curve for a "typical" (general population adult male) human and deriving the distribution of particle mass deposited in the lung. This is shown in the sequence of graphs in Figure 10-47. The mass distribution of the ambient aerosol (Figure 10-47a) is combined with the deposition efficiency curve (Figure 10-47b; similar to Figure 10-39) to obtain the thoracic mass deposition for the ambient aerosol (Figure 10-47c). The corresponding process for collection with a PM_{10} sampler is also shown. Figure 10-47a (ambient mass distribution) is combined with the sampler efficiency curve (Figure 10-47d), resulting in Figure 10-47e, which shows the collected mass distribution for the ambient aerosol. If Figure 10-47c is superimposed on Figure 10-47e, figures such as 10-48 and 10-49 will be generated.

Figures 10-48 and 10-49 illustrate the fractional mass deposition seen with representative ambient aerosols for the cities of Phoenix and Philadelphia. These trimodal aerosols were described in Chapter 3, and their parameters are provided in Appendix 10C. From these graphs it is shown that the $PM_{2.5}$ sampler distribution accounts for the particle mass in the fine (<1.0 μm) mode and the transition mode (MMAD ~2.5 μm) but does not account for the smaller mass of coarse mode particles that would be deposited in the thorax (mainly affecting tracheobronchial deposition in mouth breathers). Failure of the $PM_{2.5}$ sampler to account for coarse mode particle thoracic deposition is more evident for the Phoenix aerosol than for the Philadelphia aerosol.

Because mass deposition is not the only dose metric that is of interest, a similar modeling exercise was conducted for particle number, using the Philadelphia and Phoenix aerosols. Simulations were again performed with parameters for adult males and a general population activity pattern. Figure 10-50 shows the predicted fraction of total number of particles inhaled that is deposited in each region of the respiratory tract (ET, TB, A) for the Philadelphia aerosol. Figure 10-51 shows the number of particles deposited each day in each respiratory tract region for the Philadelphia aerosol assuming an exposure to a total particulate mass concentration of 50 $\mu g/m^3$. These figures show that a large fraction of the number of deposited particles is contributed, as anticipated, by the fine fraction mode, and that this can represent a very large number of particles deposited per day (on the order of 100,000,000) in the alveolar region. Figure 10-52 shows the predicted fraction of total number of particles inhaled that is deposited in each respiratory tract region for the Phoenix aerosol, and Figure 10-53 shows the number of

particles deposited each day in each respiratory tract region for this aerosol assuming an exposure to a total particulate mass concentration of 50 μg/m^3. The more disperse intermodal fraction of the Phoenix aerosol (see Figure 10C-2 in Appendix 10C) contributes more particles to the fine mode size-range than that of the Philadelphia aerosol.

Hygroscopic Aerosols

The ICRP66 (1994) deposition model as so far described relates to the distribution of activity or mass of aerosol particles with respect to their size on entering the respiratory tract. However, in the case of a hygroscopic material, it is necessary to take account of the increase in particle size that occurs when such materials are exposed to the near-saturated air in the respiratory tract. The ICRP66 model can be applied for hygroscopic materials by replacing the values of particle aerodynamic diameter, d_{ae}, and diffusion coefficient, D, in ambient air with the values $d_{ae}(j)$ and D_j attained in each region, j, of the respiratory tract.

Annexe D of ICRP66 describes how the growth of a hygroscopic particle can be approximated in general terms as a function of its residence time in saturated air at body temperature. For a residence time, t_j^r, in region, j, measured from inspiration of the particle (*i.e.*, entry to the nose or mouth), the particle aerodynamic diameter and diffusion coefficient attained by hygroscopic growth are approximately related to $d_{ae}(0)$ and D(0), the respective values in ambient air (*i.e.*, the external environment), and the values at equilibrium, $d_{ae}(\infty)$ and $D(\infty)$ are

$$d_{ae}(t_j^r) = d_{ae}(\infty) - [d_{ae}(\infty) - d_{ae}(0)] \exp\left(-\{10\, t_j^r\}^{0.55} \left[\frac{D(0) - D(\infty)}{d_{ae}(0)}\right]\right)^{0.6}, \text{ and} \qquad (10\text{-}58)$$

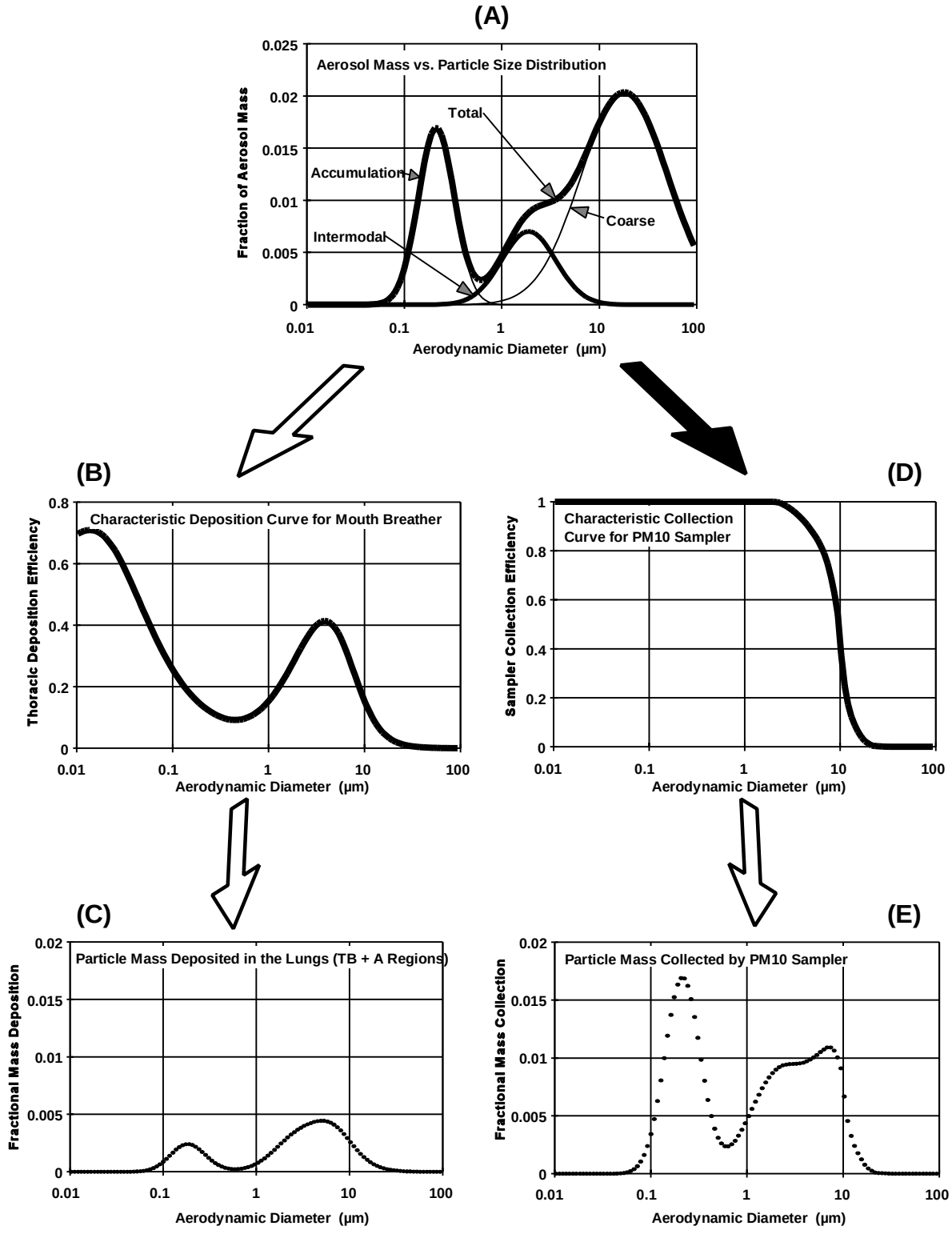

Figure 10-47. Schematic illustration of how ambient aerosol distribution data were integrated with respiratory tract deposition efficiency (using 1994 ICRP66 model) or sampler efficiency to calculate deposition in respiratory tract regions or mass collected by sampler.

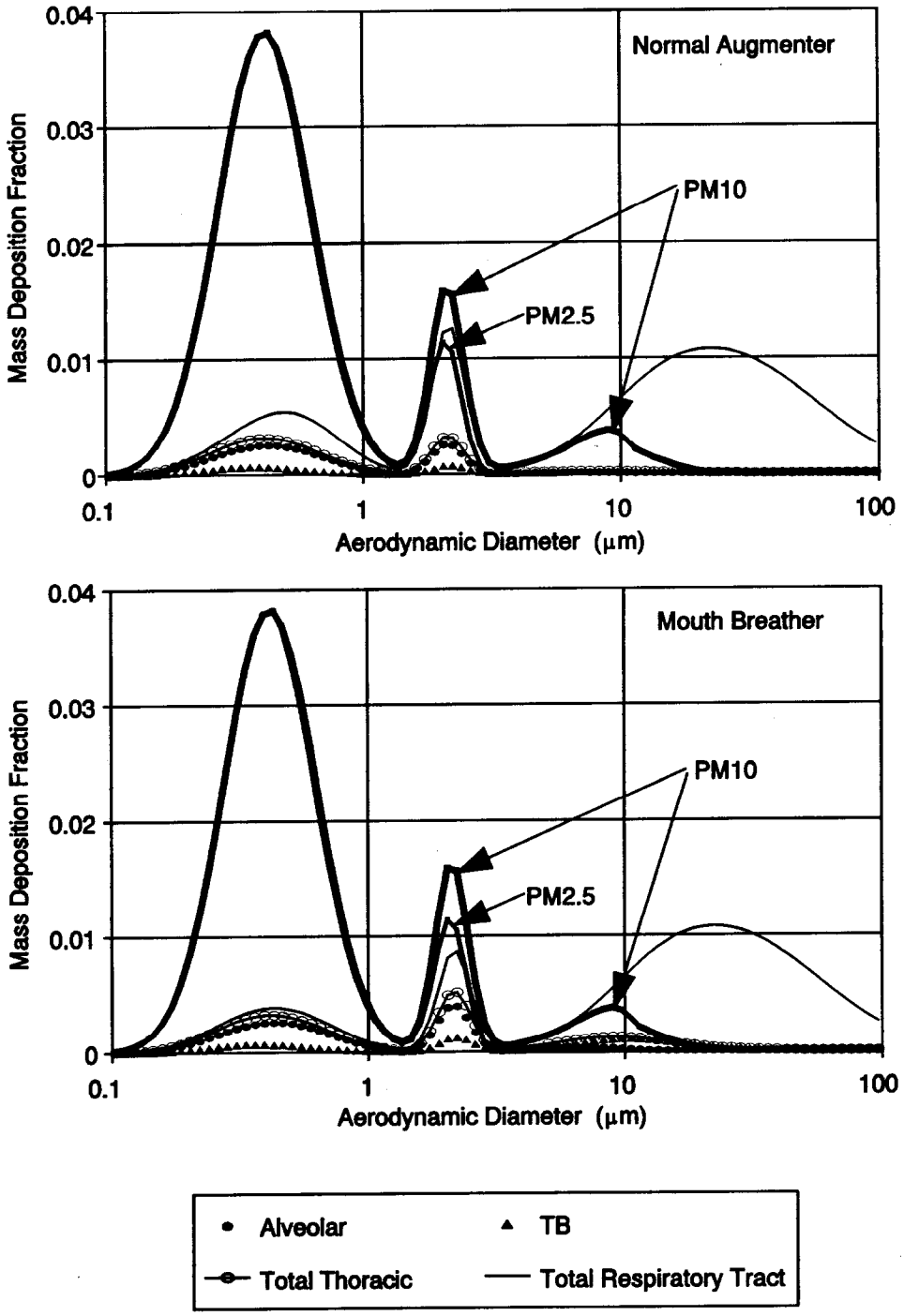

Figure 10-48. Mass deposition fraction in normal augmenter versus mouth breather adult male with a general population minute volume activity pattern predicted by the International Commission on Radiological Protection Publication 66 (1994) model and the mass collected by PM_{10} or $PM_{2.5}$ samplers for Philadelphia aerosol (described in Appendix 10C).

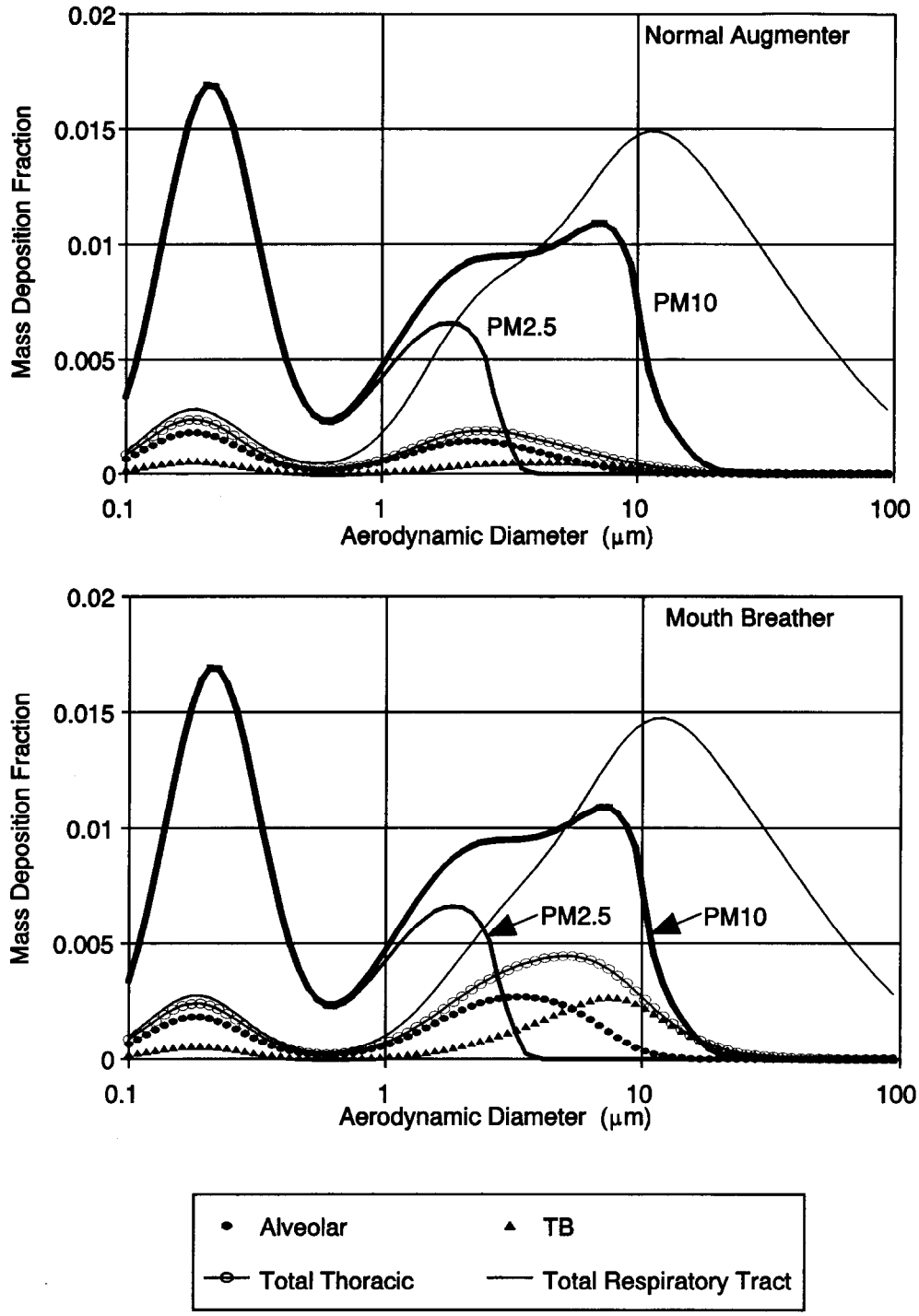

Figure 10-49. Mass deposition fraction in normal augmenter versus mouth breather adult male with a general population minute volume activity pattern predicted by the International Commission on Radiological Protection Publication 66 (1994) model and the mass collected by PM_{10} or $PM_{2.5}$ samplers for Phoenix aerosol (described in Appendix 10C).

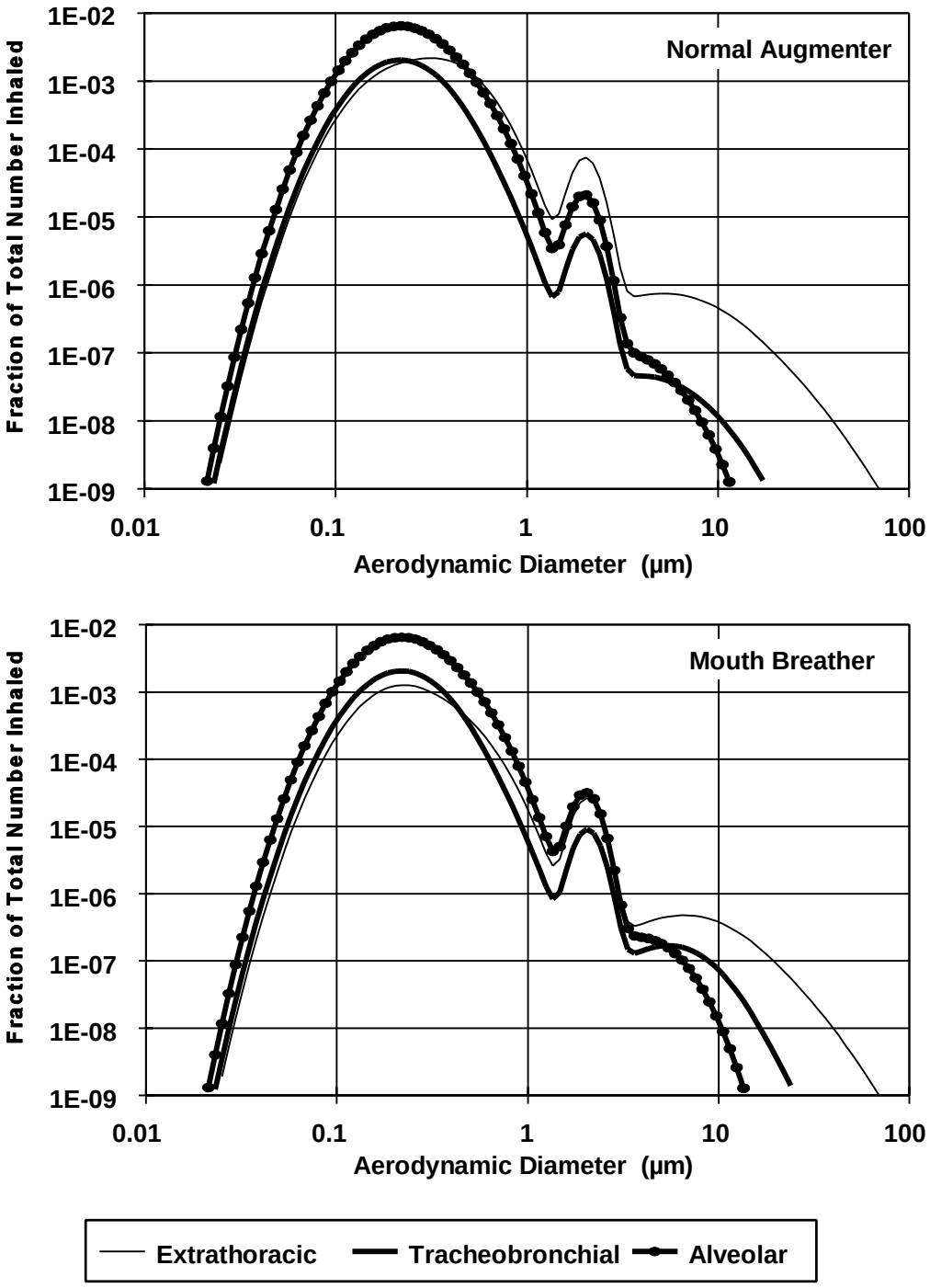

Figure 10-50. Fractional number deposition in each respiratory tract region for normal augmenter versus mouth breather adult male with a general population activity pattern as predicted by the International Commission on Radiological Protection Publication 66 (1994) model for an exposure to the Philadelphia aerosol (described in Appendix 10C).

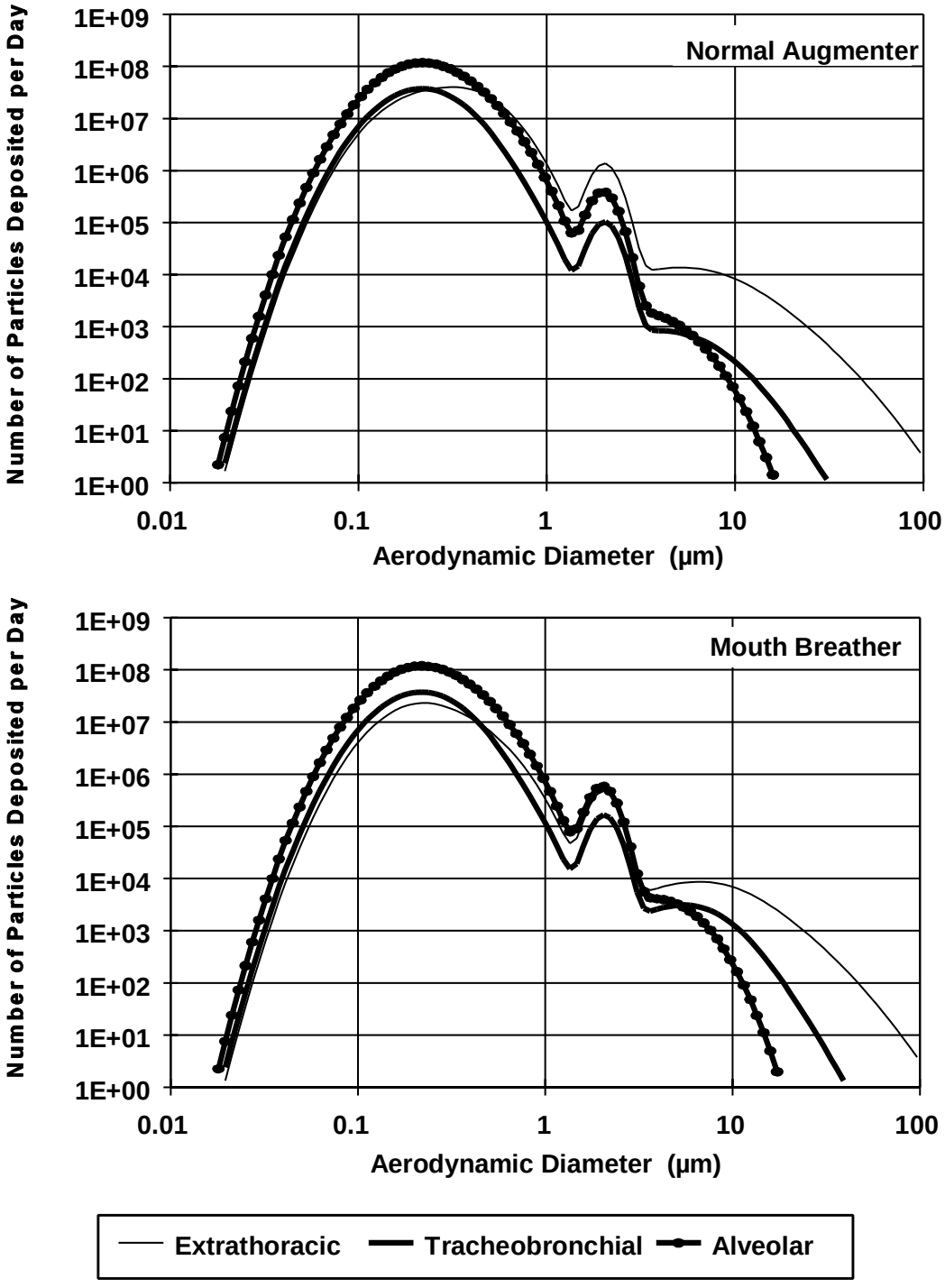

Figure 10-51. Number of particles deposited per day in each respiratory tract region for normal augmenter versus mouth breather adult male with a general population activity pattern as predicted by the International Commission on Radiological Protection Publication 66 (1994) model for an exposure to the Philadelphia aerosol (described in Appendix 10C) at a concentration of 50 μg/m^3.

To solve the model for a specific material, it is necessary to specify the degree of particle size growth at equilibrium. This generally lies in the range of two- to fourfold growth, depending on the amount of hygroscopic material associated with the particle. However, ICRP66 suggests that it is likely to be adequate to assume by default a threefold growth factor at equilibrium, for substitution in these equations. Note that the initial aerodynamic diameter, $d_{ae}(0)$, is increased by particle growth, whereas the initial diffusion coefficient, D(0), is decreased.

The effect of hygroscopic particle growth is generally to decrease total lung deposition for submicron-sized particles, and to increase it for larger particles. As discussed in some detail in Annexe D of ICRP66, the particle size in ambient air corresponding to minimum lung deposition is reduced from about 0.4 μm for non-hygroscopic particles to about 0.1 μm for hygroscopic particles (Tu and Knutson, 1984; Blanchard and Willeke, 1984).

Intrahuman Variability in Regional Deposition

The experimental data on regional deposition of particles in the human respiratory tract indicate substantial intersubject variability, even if the particles are inhaled under identical exposure conditions. In ICRP66, the upper and lower 95% confidence bounds of the data are represented by a variable coefficient, a, which is incorporated into each algebraic expression for deposition efficiency (see ICRP66, Chapter 5, Tables 12 and 13, pp. 45 and 46). In each case, the coefficient is taken to be log-normally distributed, (i.e., $a_{upper} = a_{median} \times \sigma_g^2$, and $a_{lower} = a_{median} \div \sigma_g^2$) where σ_g is the fitted geometric standard deviation. Other confidence bounds on the predicted regional deposition efficiency are given by substituting an appropriate value of the coefficient, a, that is sampled from the defined log-normal distribution.

Representing the median (or expectation) value of the coefficient, a, for each region, j, by a_j, then it is convenient to use a dimensionless scaling constant, c_j, as a multiplier or divisor of the median value. In Table 14 of ICRP66 (Chapter 5, p. 49), the ICRP gives values of this scaling constant that are estimated to describe the spread in the experimental data for regional respiratory tract deposition. The scaling factors defining the upper and lower 95% confidence bounds of regional deposition range from × or ÷ by 1.4 in the expression for "thermodynamic" deposition efficiency of the extrathoracic (ET) region, to × or ÷ by 3.3 for the "aerodynamic" deposition efficiency of the ET region. To evaluate the uncertainty distribution of the predicted deposition fractions in all five regions of the respiratory tract (i.e., ET_1, ET_2, BB, bb, and AI) it is necessary to select the respective values of c_j at random from their assumed log-normal distributions.

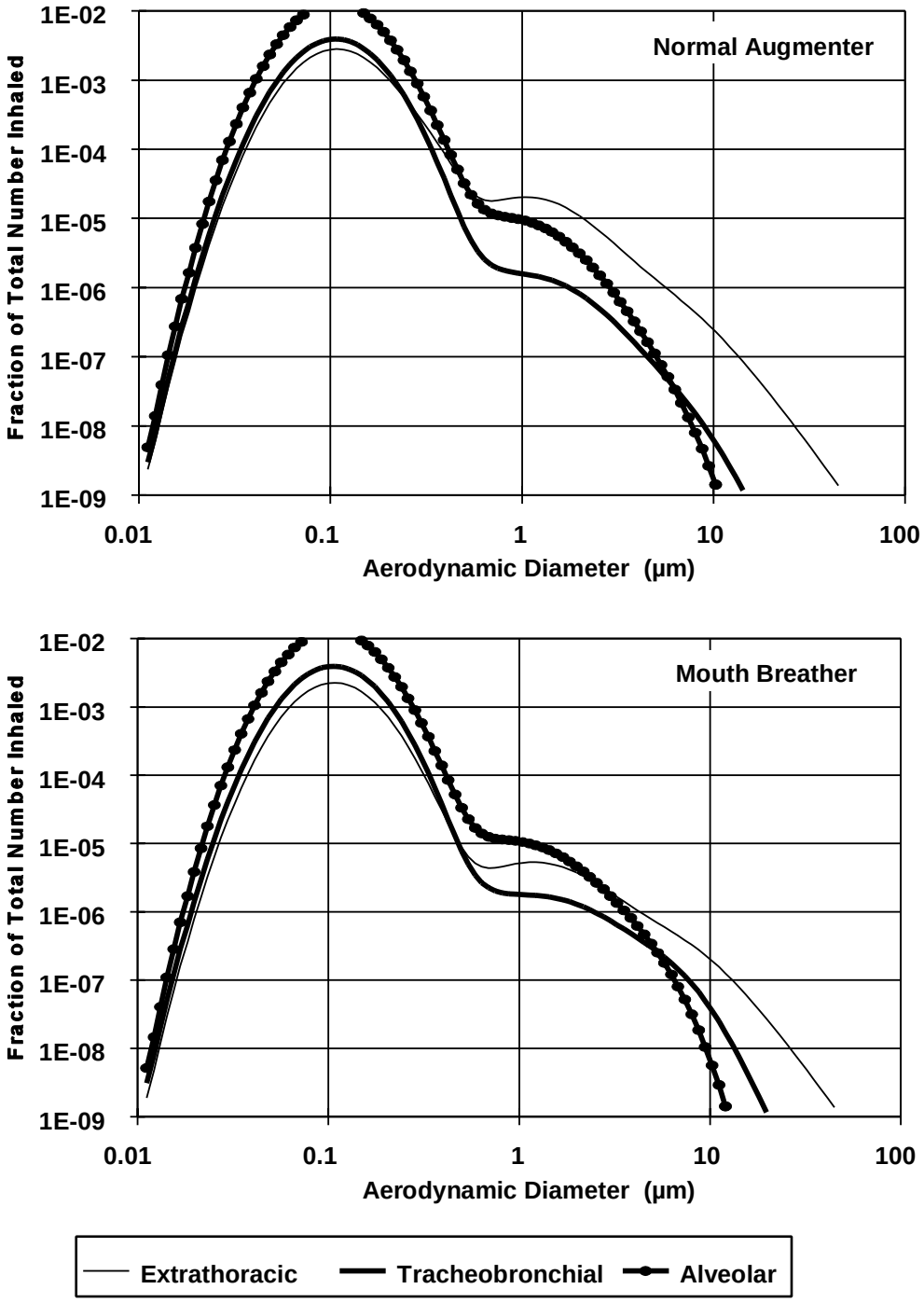

Figure 10-52. Fractional number deposition in normal augmenter versus mouth breather adult male with a general population activity pattern predicted by the International Commission on Radiological Protection Publication 66 (1994) model for an exposure to the Phoenix aerosol (described in Appendix 10C).

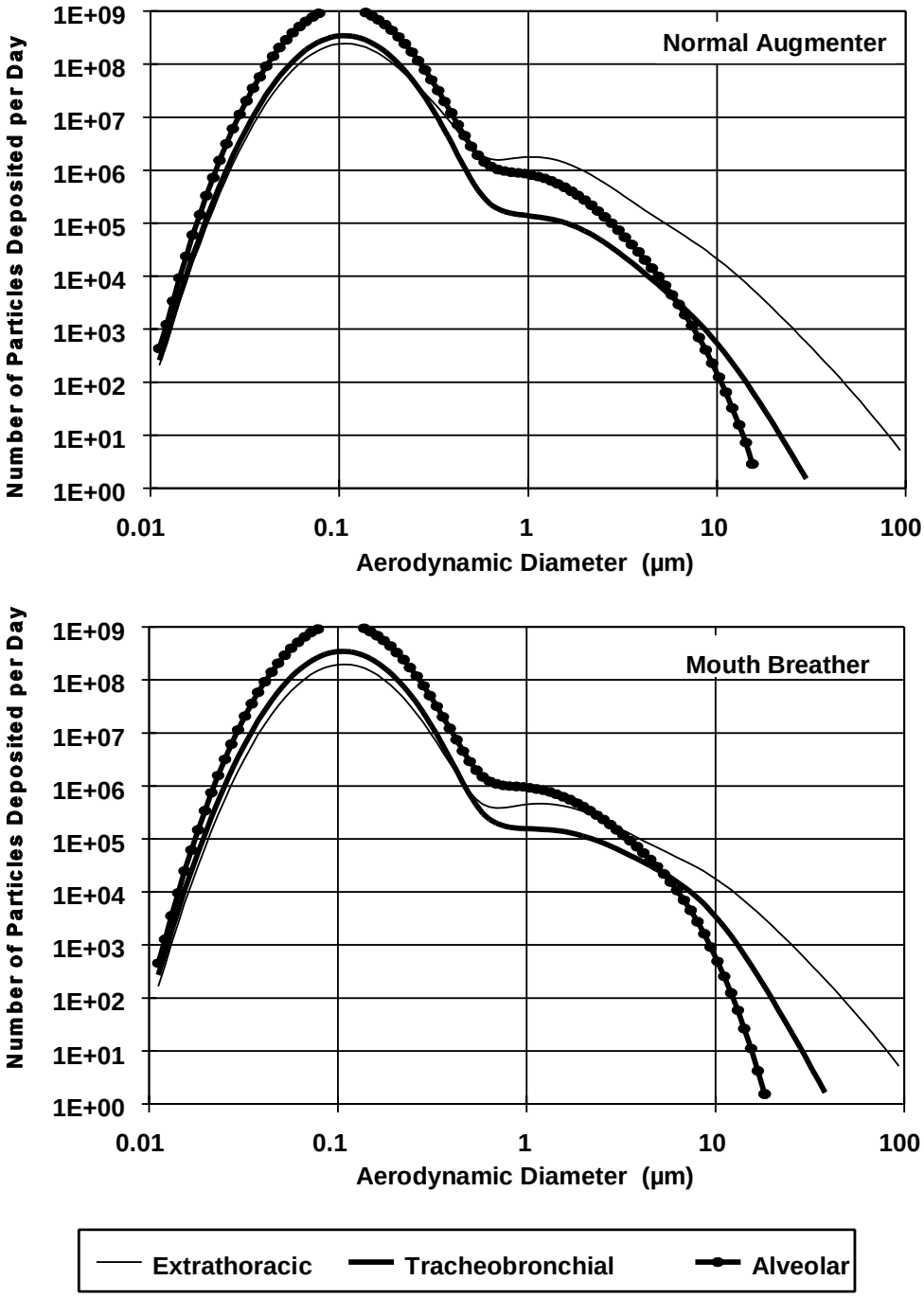

Figure 10-53. Number of particles deposited per day in each respiratory tract region for normal augmenter versus mouth breather adult male with a general population activity pattern predicted by the International Commission on Radiological Protection Publication 66 (1994) model for an exposure to the Phoenix aerosol (described in Appendix 10C) at a concentration of 50 μg/m^3.